

BACHELOR

Coarse-graining of density functional theory

Verhoeven, Lieke M.

Award date:
2019

[Link to publication](#)

Disclaimer

This document contains a student thesis (bachelor's or master's), as authored by a student at Eindhoven University of Technology. Student theses are made available in the TU/e repository upon obtaining the required degree. The grade received is not published on the document as presented in the repository. The required complexity or quality of research of student theses may vary by program, and the required minimum study period may vary in duration.

General rights

Copyright and moral rights for the publications made accessible in the public portal are retained by the authors and/or other copyright owners and it is a condition of accessing publications that users recognise and abide by the legal requirements associated with these rights.

- Users may download and print one copy of any publication from the public portal for the purpose of private study or research.
- You may not further distribute the material or use it for any profit-making activity or commercial gain

Coarse-Graining of Density Functional Theory

Bachelor End Project

L.M. Verhoeven
student number 0992218

July 4, 2019

Committee members:

dr. B. Baumeier

dr. ir. M.J.H. Anthonissen

ir. W.L.J. Scharpach

Abstract

In this thesis, the theoretical framework behind Density Functional Theory (DFT) and a new approach of DFT, called Coarse-Graining Density Function Theory (CGDFT), is discussed. CGDFT will be discussed in general and a practical numerical implementation is applied to single atoms. Standard DFT is a technique to obtain the minimum total energy (ground-state) of a system of interacting nuclei and electrons without solving the many-body Schrödinger equation of quantum mechanics directly. Typically, this energy in DFT is determined from a set of eigenvalues and eigenvectors of its Hamiltonian. The key idea of CGDFT is that the ground-state energy does not depend on individual eigenvalues and eigenvectors of the DFT Hamiltonian, but on their collective effects, respectively the band-structure energy and the electron density. After sampling and weighting the involved sums, a linear scaling method using a Gaussian quadrature will be used to evaluate the electron density. Next, in the coarse-graining step, a spatial approximation scheme is used to obtain a high-accurate density approximation where necessary. In this thesis, a reformulation of CGDFT is given for single atoms. For single atoms, there is only one nucleus, so we can place the origin there and we do not have to take nucleus-nucleus interactions into account. When using a 3D difference approximation scheme for the Laplacian and Riemann sums to evaluate the integrals of the potentials, the ground-state energy can be approximated. For helium, the experimental ground-state energy is -2.9... Ha and the CGDFT approximation of it is -2.7491 Ha; the difference is mainly caused by the choice for the pseudo-potential, the Evanescent pseudo-potential, and the usage of the LDA approximation for the exchange-correlation energy. Because of this result, one is led to think that CGDFT gives a fairly good approximation for the ground-state energy.

Contents

1	Introduction	3
2	Introduction to quantum mechanics	4
2.1	The wave function and the state space	4
2.2	The Schrödinger equation	5
2.3	Quantum observables	7
2.3.1	Heisenberg's representation	8
2.3.2	Schrödinger's representation	10
2.4	Spin	11
2.5	Comparison of quantum mechanics with classical mechanics	12
2.6	The uncertainty principle	12
2.7	Spectrum and dynamics	13
2.8	The many-particle system in \mathbb{R}^3	14
2.9	Summary	15
3	The hydrogen atom	16
3.1	Proof of Theorem 6	19
3.2	Example of a radial wave function	21
3.3	Energy states	22
4	Electronic structure theory of many-electron systems	25
4.1	The Born-Oppenheimer approximation	26
4.2	The Hartree-Fock method	27
4.3	Density Functional Theory	29
4.4	Exchange-correlation energy approximations	33
4.5	Summary	34
5	Application of DFT to single atoms	35
6	Coarse-Graining Density Functional Theory	39
6.1	The key idea of the reformulation of DFT	40
6.2	Linear-Scaling Spectral Gaussian Quadrature Method	42
6.3	Formulation of CGDFT	45
6.4	CGDFT on single atoms	46
6.5	CGDFT on a helium atom	50
7	Conclusion	53
8	Discussion	54
	References	55
	Appendices	57
A	Matlab program CGDFT on atoms	57

1 Introduction

A lot of today's technology, for example computers and smartphones, makes use of *silicon wafers*. A silicon wafer is a thin slice of a silicon material that serves as a semiconductor, with a thickness between 200 and 300 μm . The silicon wafers are mostly used as integrated circuits, which power the devices. Another usage of silicon wafers, however, is inside solar cells, in which the wafers absorb photons from the sunlight and in return create electricity. It is important that the wafers are (nearly) free of any defects. If they are not, electronic properties of the silicon change, even when the defects are present in small numbers. An example of a defect is a *vacancy*, which is the absence of an atom in the molecular structure of the silicon, depicted in Figure 1. To explore how the structure changes, the energy distribution among the particles can be investigated. In order to do so, a mathematical approximation of the electronic structure can be used. For this approximation, we need quantum mechanics.

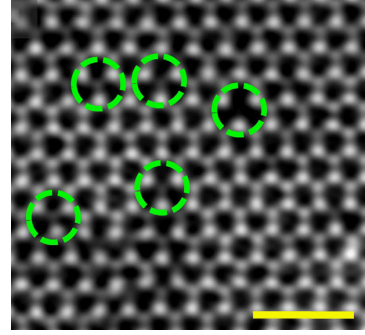


Figure 1: *Vacancies in a layer of atoms.* Source: [Schrit]

So, first, a brief overview of quantum mechanics will be given in Chapter 2, with the necessary mathematical background as well. The most important equation here is the *Schrödinger equation* and its associated eigenvalue problem, as its eigenvalues give the energies we want to investigate. The minimal energy is the *ground-state energy*. The minimization of this energy can be done analytically only for a few cases. One of these is the hydrogen atom, which will be discussed in Chapter 3. For large *many-electron systems*, this is no longer possible and the energies can only be obtained numerically. There are different ways to approximate the electronic structure of these systems, which will be discussed in Chapter 4. From the different approaches, Density Functional Theory (DFT) is the most popular. Here, the many-body problem is formulated in terms of the observable *electron density* instead of the unobservable individual contribution of the electrons. In Chapter 5, a formulation of DFT applied to the carbon atom will be discussed. However, considering the long-range effects of a defect, DFT is computationally expensive, and a refined approach is needed. In order to speed up the analysis of defects in materials, a reformulation of DFT will be presented in this Chapter 6, called *Coarse-Graining Density Functional Theory* (CGDFT). First, a linear scaling method is used, which directly evaluates the electron density. Next, a spatial approximation scheme is used, choosing representative nodes and interpolating through the non-representative nodes. CGDFT is especially developed for large molecules, but in Chapter 6 I will reformulated it for single atoms. After the reformulation, it will be investigated whether or not CGDFT also gives a good approximation for the ground state energy of helium. Also, how sensitive this approach is to computational parameters will be investigated.

2 Introduction to quantum mechanics

Quantum mechanics started with the thoughts developed by Max Planck. His idea was that electro-magnetic radiation is emitted and absorbed in discrete amounts, which are called *quanta*. Einstein investigated this in more detail, and suggested that electro-magnetic radiation itself consists of particles, which are called *photons*. The quantum and the photon were the first two discovered quantum particles, and by this also the first glimpse of the *wave-particle duality* in quantum mechanics was obtained. After this, Bohr devised a new quantum mechanical model of an atom, in which the electrons orbit around the nucleus in fixed states, and can jump from one orbit to the other. This model led to *Heisenberg* and *Schrödinger quantum mechanics* [Gustafson and Sigal2011].

Two important experiments have been carried out at the beginning of quantum mechanics. The first one was conducted by Rutherford in 1911, and revealed that the weight of an atom is concentrated in the nucleus, with the electrons orbiting around it. Also, it showed that the electrons are attracted by the nucleus and repelled by each other, due to Coulomb forces. This was in accordance with Bohr's model. The second experiment investigated the scattering behaviour of electrons in a crystal, which could be compared to the *double-slit experiment*. In the double-slit experiment, a light source illuminates a plate, which is equipped with two parallel slits. The light, passing through the slits, is observed behind the plate on a screen. Since light has wave-like properties, it shows an interference pattern when passing through the slits.[Young, Chapter 35] This pattern would not be observed if light would solely consist of particles. The same experiment was conducted with electrons, where on the screen, a similar interference pattern of the electrons was observed. From this last experiment, two important observations have been obtained: individual electrons behave randomly, and they have wave-like properties. Quantum mechanics arose from the observations that could not be explained in classical mechanics. A mathematical framework was needed, on which Schrödinger, Heisenberg, Born and others worked. In this chapter, a brief overview of quantum mechanics will be given, with the necessary mathematical background information.

2.1 The wave function and the state space

In a quantum mechanical model, the state of a particle is identified by a function of its position $x \in \mathbb{R}^d$ and time $t \in \mathbb{R}_0^+$. This function is called the *wave function* or *state*, and is denoted by $\psi = \psi(x, t)$. Such a function should satisfy the following properties:

- $|\psi(\cdot, t)|^2$ is a continuous probability distribution, which describes the probability of finding a particle at position x , as a function x (of the position of the particle) at any time $t \in \mathbb{R}_0^+$.
- The function $\psi(\cdot, t)$ should satisfy some sort of wave equation for any time $t \in \mathbb{R}_0^+$.

The space of all possible states of the particles for a given time $t \in \mathbb{R}_0^+$ is the *state space*, which in this report is the space of square-integrable functions over the position spaces $x \in \mathbb{R}^d$, where $L^2(\mathbb{R}^d) = L^2(\mathbb{R}^d; \mathbb{C}^n)$:

$$L^m(\mathbb{R}^d; \mathbb{C}^n) := \left\{ f : \mathbb{R}^d \rightarrow \mathbb{C}^n \mid \int_{\mathbb{R}^d} |f(x)|^m dx < \infty \right\} \quad m, n \in \mathbb{N},$$

2. INTRODUCTION TO QUANTUM MECHANICS

in which $L^m(\mathbb{R}^d; \mathbb{C}^n)$ will be shortened to $L^m(\mathbb{R}^d)$. For $m = 2$, these spaces are *Hilbert spaces* for all n . Note that state space is for $m = 2$ and not for general m .

Definition 1. *The space \mathcal{H} is a Hilbert space if the map*

$$\langle \cdot, \cdot \rangle : \mathcal{H} \times \mathcal{H} \rightarrow \mathbb{C},$$

which is called the inner product, satisfies the following properties for all $v, w, z \in \mathcal{H}$:

- *linearity in the second argument:* $\langle v, \alpha w + \beta z \rangle = \alpha \langle v, w \rangle + \beta \langle v, z \rangle$ for all $\alpha, \beta \in \mathbb{C}$;
- *conjugate symmetry:* $\langle w, v \rangle = \overline{\langle v, w \rangle}$;
- *positive definiteness:* $\langle v, v \rangle > 0$ for $v \neq 0$.

For $f, g \in L^2(\mathbb{R}^d)$, the inner product is defined by

$$\langle f, g \rangle_{L^2(\mathbb{R}^d)} := \int_{\mathbb{R}^d} \overline{f(x)} g(x) d^d x.$$

2.2 The Schrödinger equation

The *Schrödinger equation*¹ governs the evolution of the wave function of the particle, and has the following properties:

- *Causality:* The state $\psi(x, t_0)$ at $t = t_0$ should determine the states $\psi(x, t)$ for all $t > t_0$;
- *Superposition principle:* if $\xi(x, t)$ and $\phi(x, t)$ are evolutions of states, than $\alpha \xi(x, t) + \beta \phi(x, t)$, for $\alpha, \beta \in \mathbb{C}$, should describe the evolution of a state, too;
- *Correspondence principle:* In “everyday” situations, quantum mechanics should be in correspondence with classical mechanics. An example of this is the momentum, which will be discussed later on.

The general *Schrödinger equation* is given by

$$i\hbar \frac{\partial}{\partial t} \psi = H\psi, \tag{1}$$

in which H is a linear *Schrödinger operator*, which operates on wave functions ψ , and is also called the *Schrödinger Hamiltonian* or simply *Hamiltonian*. A Hamiltonian in quantum mechanics, is an operator, which corresponds to the potential energies and the sum of the kinetic energy of all particles in a system. Furthermore, \hbar is the *reduced Planck constant* which is $\hbar := \frac{h}{2\pi} = 3.16152649 \cdot 10^{-26} \text{ J} \cdot \text{m}$. The Schrödinger Hamiltonian is given by

$$\begin{aligned} H\psi(x, \cdot) &: L^2(\mathbb{R}^d) \rightarrow L^2(\mathbb{R}^d), \\ \psi &= \psi(x, \cdot) \mapsto H\psi(x, \cdot) \\ H &:= \left(-\frac{\hbar^2}{2m} \Delta_x + \mathcal{V} \right) \psi(x, \cdot) = -\frac{\hbar^2}{2m} \Delta_x \psi(x, \cdot) + V(x) \psi(x, \cdot). \end{aligned} \tag{2}$$

¹The Schrödinger equation is named after Erwin Schrödinger. The equation was derived in 1925, and he published it in 1926, which formed the basis for the work that resulted in his Nobel Prize in Physics in 1933.

2. INTRODUCTION TO QUANTUM MECHANICS

Here, \mathcal{V} is a *potential multiplication operator* (corresponding to the potential function $V = V(x)$), which in such a system has the meaning: “it gives the amount of work needed in order to move a particle of positive charge from a reference point to a specific point inside the field without producing acceleration”. [Wikipedia2010] Some examples of potential operators are the following:

- *Free motion*: $V \equiv 0$;
- *The double-slit experiment*: $V \equiv \infty$ on the plate and $V \equiv 0$ else;
- *The Coulomb potential*: $V(x) = -\frac{e^2}{|x|}$, which we will encounter later in Chapter 3 on the hydrogen atom.

When adding to (1) an initial condition

$$\psi(x, 0) = \psi_0(x) \quad \text{for some } \psi_0 \in L^2(\mathbb{R}^d), \quad (3)$$

(1) and (3) together form an initial value problem (IVP).

For the Schrödinger operator H , it is important that the probability $|\psi(x, t)|^2$ is conserved for solutions $\psi = \psi(x, t)$ of (1). This is true if and only if H is symmetric.

Definition 2. A linear operator A acting on a Hilbert space \mathcal{H} is symmetric if

$$\langle A\psi, \phi \rangle = \langle \psi, A\phi \rangle$$

for any two elements $\psi, \phi \in D(A) \subseteq \mathcal{H}$.

The proof of this can be found in [Gustafson and Sigal2011, Chapter 2]. In this proof, we compute $\frac{d}{dt} \langle \psi, \psi \rangle$ and use that if H is symmetric, its time-derivative is zero. An important symmetric operator on $L^2(\mathbb{R}^d)$ is the *Schrödinger operator with free motion* (so $V \equiv 0$), which we call

$$H_0 := -\frac{\hbar^2}{2m} \Delta_x. \quad (4)$$

It can be proven in a straight-forward way that this operator is indeed symmetric, by using both integration by parts and the rapid decay of wave functions twice:

$$\begin{aligned} \left\langle -\frac{\hbar^2}{2m} \Delta_x \psi, \phi \right\rangle_{L^2(\mathbb{R}^d)} &= -\frac{\hbar^2}{2m} \int_{\mathbb{R}^d} \overline{\Delta_x \psi(x)} \phi(x) d^d x = -\frac{\hbar^2}{2m} \sum_{i=1}^d \int_{\mathbb{R}^d} \overline{\partial_{x_i}^2 \psi(x)} \phi(x) d^d x \\ &= -\frac{\hbar^2}{2m} \sum_{i=1}^d \int_{\mathbb{R}^d} \overline{\psi(x)} \partial_{x_i}^2 \phi(x) d^d x = \left\langle \psi, -\frac{\hbar^2}{2m} \Delta_x \phi \right\rangle_{L^2(\mathbb{R}^d)}. \end{aligned}$$

The operators that will be investigated in the quantum mechanics setting are not only symmetric, but also *self-adjoint*. The self-adjointness in quantum mechanics can be seen as an analogy of real symmetric matrices, when these matrices are seen as operators. From now on, we assume that each H is symmetric.

Definition 3. A linear operator A acting on a Hilbert space \mathcal{H} is self-adjoint if A is symmetric and the equation $(A \pm i)\psi = f$ has solutions $\psi \in \mathcal{H}$ for all $f \in \mathcal{H}$.

The self-adjointness of an operator proves existence of the *dynamics*.

Definition 4. The dynamics exist if for all $\psi_0 \in \mathcal{H}$, the IVP (1) and (3) has a unique solution ψ which conserves probability.

For H_0 , given in (4), self-adjointness on $L^2(\mathbb{R}^3)$ will be proven. Symmetry has already been proven, so we prove, using a *Fourier transform*, that for every $f \in \mathcal{H}$ there are solutions $\psi \in \mathcal{H}$ to the equation

$$\left(-\frac{\hbar^2}{2m}\Delta_x + i\right)\psi = f. \quad (5)$$

Definition 5. The Fourier transform, $\mathcal{F} : L^1(\mathbb{R}^d) \rightarrow L^1(\mathbb{R}^d)$, maps a function $\psi \in L^1(\mathbb{R}^d)$ to another function $\hat{\psi} := \mathcal{F}[\psi] \in L^1(\mathbb{R}^d)$, where for $k \in \mathbb{R}^d$

$$\hat{\psi}(x) = \mathcal{F}[\psi](x) = (2\pi\hbar)^{-d/2} \int_{\mathbb{R}^d} e^{-ik \cdot x/\hbar} \psi(x) dx.$$

The inverse Fourier transform is given by

$$\psi(x) = \mathcal{F}^{-1}[\hat{\psi}](x) := (2\pi\hbar)^{-d/2} \int_{\mathbb{R}^d} e^{ik \cdot x/\hbar} \hat{\psi}(k) dk.$$

We have that (5) is equivalent to $\frac{1}{2m}(|k|^2 + i)\hat{\psi}(k) = \hat{f}(k)$ for all $k \in \mathbb{R}^3$. [Gustafson and Sigal 2011, Problem 23.78]

For the final step, we make use of the characterization of *Sobolev spaces*.

Definition 6. Sobolev spaces $H^n(\mathbb{R}^d) \subset L^2(\mathbb{R}^3)$, the spaces of functions containing all derivatives up to order n lying in $L^2(\mathbb{R}^d)$, and are characterized using the Fourier transform by

$$\psi \in H^n(\mathbb{R}^d) \Leftrightarrow \int_{\mathbb{R}^d} (1 + |k|^{2n}) |\hat{\psi}(k)|^2 dk < \infty.$$

Now re-writing $|\hat{f}(k)|^2 = \overline{\hat{f}(k)} \hat{f}(k)$, we have $\frac{1}{4m^2} (1 + |k|^4) |\hat{\psi}(k)|^2 = |\hat{f}(k)|^2$. By the characterization of Sobolev spaces, we find that ψ lies in $H^2(\mathbb{R}^3)$ and because of this, are solutions if and only $\psi \in H^2(\mathbb{R}^3)$. Now by Definition 3, we have that H_0 is self-adjoint. \square

2.3 Quantum observables

In the previous section, self-adjoint operators have been investigated. In quantum mechanics, such operators are called *observables*, since they can be observed in the sense that they can be measured experimentally when given in a physical framework.

Definition 7. Observables are operators which are self-adjoint on the state space $L^2(\mathbb{R}^d)$.

Recall that a continuous probability distribution is given by $|\psi(\cdot, t)|^2$. The average of position is the mean value,

$$\langle x \rangle_\psi := \langle \psi, x_j \psi \rangle = \int_{\mathbb{R}^d} x |\psi(\cdot, t)|^2 dx$$

This inspires the following expansion to general operators:

Definition 8. The average of an operator A on \mathcal{H} with respect to a state $\psi \in \mathcal{H}$ is given by

$$\langle A \rangle_\psi := \langle \psi, A\psi \rangle$$

The reason why the self-adjointness of observables is so important in quantum mechanics will be seen in the formulations of quantum mechanics by Heisenberg and Schrödinger, sometimes referred to as *representations*. For chronological reasons, the Heisenberg representation will be described first. The difference between these two formulations is the way of dealing with the time-dependence of observables: in Heisenberg's picture, the wave function is stationary, and the operators transform and evolve in time. In transforming the operators, the eigenfunctions are left unchanged. In Schrödinger's picture, however, the operators are stationary, and the eigenfunctions evolve in time, leaving the operators unchanged. [Gustafson and Sigal2011]

2.3.1 Heisenberg's representation

For the Heisenberg² representation, define the time-dependent observable $A(t)$ by

$$A(t) := e^{itH/\hbar} A e^{-itH/\hbar},$$

in which A is an operator, H a Hamiltonian and the power series representation $e^A := \sum_{n=0}^{\infty} \frac{A^n}{n!}$ is used. Furthermore, let

$$\psi(x, t) = e^{-itH/\hbar} \psi_0(x),$$

solve IVP (1) and (3). For any observable B , $e^{-itB/\hbar}$ belongs to the operator family, which consists of *evolution operators* $U(t) := e^{-it\tilde{B}}$ satisfying $i\frac{\partial \psi}{\partial t} = \tilde{B}\psi$.

Theorem 1. *If B is a self-adjoint operator on \mathcal{H} , there is a unique family of bounded, time-dependent operators $U(t) := e^{itB}$ having the following properties for $s, t \in \mathbb{R}$:*

$$\begin{aligned} i\frac{d}{dt}U(t) &= BU(t) = U(t)B, \\ U(0) &= \text{Id and } U(t)\psi \xrightarrow{t \rightarrow 0} \psi, \text{ for } t \rightarrow 0, \\ U(t)U(s) &= U(t+s), \\ \|U(t)\psi\| &= \|\psi\|. \end{aligned}$$

A proof of this can be found in [Suryanarayana et al.2013, Chapter 2] in which the power series representation is used. Some computations for the average show the following:

Lemma 1. *For all t , $\langle B \rangle_{\psi(t)} = \langle B(t) \rangle_{\psi_0}$.*

Proof:

$$\begin{aligned} \langle B \rangle_{\psi(t)} &= \langle \psi(t), B\psi(t) \rangle = \langle e^{-itH/\hbar} \psi_0, B e^{-itH/\hbar} \psi_0 \rangle \\ &= \langle \psi_0, e^{itH/\hbar} B e^{-itH/\hbar} \psi_0 \rangle = \langle B(t) \rangle_{\psi_0}. \quad \square \end{aligned}$$

In quantum mechanics, the value of two physical values at the same time cannot be known if they do not *commute*. This is the case, for example, for position and momentum. We say that A and B commute if their commutators yields zero.

Definition 9. *The commutator of operators A and B is $[A, B] := AB - BA$.*

²The uncertainty principle was introduced first in 1927 by Werner Heisenberg, who was a German physicist.

2. INTRODUCTION TO QUANTUM MECHANICS

The equation for the time evolution of an observable can be computed by making use of the time derivative.

Lemma 2. *The time evolution of an observable $A(t)$ is given by*

$$\frac{d}{dt}A(t) = \frac{i}{\hbar} [H, A(t)],$$

which is also known as the Heisenberg equation.

Proof: In this proof, the power series representation of $e^A = \sum_{n=0}^{\infty} \frac{A^n}{n!}$ will be used.

$$\begin{aligned} \frac{d}{dt}A(t) &= \frac{d}{dt} \left(e^{itH/\hbar} A e^{-itH/\hbar} \right) \\ &= \frac{i}{\hbar} H e^{itH/\hbar} A e^{-itH/\hbar} + e^{itH/\hbar} A \frac{i}{\hbar} (-H) e^{-itH/\hbar} \\ &= \frac{i}{\hbar} \left(H \sum_{n=0}^{\infty} \frac{(itH/\hbar)^n}{n!} A \sum_{n=0}^{\infty} \frac{(-itH/\hbar)^n}{n!} + \sum_{n=0}^{\infty} \frac{(itH/\hbar)^n}{n!} (-AH) \sum_{n=0}^{\infty} \frac{(-itH/\hbar)^n}{n!} \right) \\ &= \frac{i}{\hbar} \left(H \sum_{n=0}^{\infty} \frac{(itH/\hbar)^n}{n!} A \sum_{n=0}^{\infty} \frac{(-itH/\hbar)^n}{n!} - \sum_{n=0}^{\infty} \frac{(itH/\hbar)^n}{n!} A \sum_{n=0}^{\infty} \frac{(-itH/\hbar)^n}{n!} H \right) \\ &= \frac{i}{\hbar} (HA(t) - A(t)H) = \frac{i}{\hbar} [H, A(t)]. \end{aligned}$$

□

From the Heisenberg equation, the quantum-analogue version of the definition of momentum in classical mechanics can be defined.

Definition 10. *The momentum operator p is defined by $|p|^2 = \sum_j p_j^2$, with*

$$p_j := -i\hbar \partial_{x_j}.$$

Classical momentum is defined by

$$p(t) := mv(t),$$

where m denotes mass and $v = \frac{dx}{dt}$.

Also, there is another, more special relationship between position x_j and momentum p_j .

Lemma 3. *The fundamental relation between the position operator x_j and the momentum operator p_j is given by*

$$[p_j, x_j] = -i\hbar.$$

Proof:

$$\begin{aligned} [p_j, x_j]\psi &= p_j x_j \psi - x_j p_j \psi = -i\hbar \frac{\partial}{\partial x_j} (x_j \psi) + x_j i\hbar \frac{\partial \psi}{\partial x_j} \\ &= -i\hbar x_j \frac{\partial \psi}{\partial x_j} - i\hbar \psi \frac{\partial x_j}{\partial x_j} + x_j i\hbar \frac{\partial \psi}{\partial x_j} = -i\hbar \psi \\ &\implies [p_j, x_j] = -i\hbar. \end{aligned}$$

When substituting $x = x(t)$ for $A(t)$, using the Hamiltonian $H = -\frac{\hbar^2}{2m}\Delta_x + V(x) = \frac{|p|^2}{2m} + V(x)$ and the lemmas above and $p = p(t)$, we get the following result □

$$\begin{aligned}
 \frac{d}{dt}x(t) &= \frac{i}{\hbar} [H, x(t)] && \text{by Lemma 2} \\
 &= \frac{i}{\hbar} \left[\frac{p(t)^2}{2m} + V(x), x(t) \right] \\
 &= \frac{i}{2\hbar m} [p(t)^2, x(t)] + \frac{i}{\hbar} [V(x), x(t)] && \text{since } V(x) \text{ and } x(t) \text{ commute } [V(x), x(t)] = 0 \\
 &= \frac{i}{2\hbar m} (p(t) [p(t), x(t)] + [p(t), x(t)] p(t)) \\
 &= \frac{i}{2\hbar m} (-i\hbar p(t) - i\hbar p(t)) = \frac{1}{m} p(t).
 \end{aligned}$$

Therefore, Heisenberg's representation of the momentum operator is in accordance with the classical momentum.

2.3.2 Schrödinger's representation

The second representation of quantum mechanics is Schrödinger's representation.

Lemma 4. *For any observable A on \mathcal{H} and any solution $\psi \in \mathcal{H}$ of (1), the following holds:*

$$\frac{d}{dt}\langle A \rangle_\psi = \left\langle \frac{i}{\hbar} [H, A] \right\rangle_\psi.$$

Proof: From the fact that ψ satisfies (1), we have $\frac{\partial \psi}{\partial t} = \frac{1}{i\hbar} H\psi$.

$$\begin{aligned}
 \frac{d}{dt}\langle A \rangle_\psi &= \frac{d}{dt}\langle \psi, A\psi \rangle = \langle \dot{\psi}, A\psi \rangle + \langle \psi, A\dot{\psi} \rangle \\
 &= \left\langle \frac{1}{i\hbar} H\psi, A\psi \right\rangle + \left\langle \psi, A \frac{1}{i\hbar} H\psi \right\rangle = \overline{\left\langle \psi, \frac{1}{i\hbar} H A\psi \right\rangle} + \left\langle \psi, A \frac{1}{i\hbar} H\psi \right\rangle \\
 &= \left\langle \psi, \frac{i}{\hbar} H A\psi \right\rangle - \left\langle \psi, \frac{i}{\hbar} A H\psi \right\rangle = \left\langle \psi, \frac{i}{\hbar} [H, A]\psi \right\rangle \\
 &= \left\langle \frac{i}{\hbar} [H, A] \right\rangle_\psi.
 \end{aligned}$$

□

We have that $\Delta_x(x\psi) = x\Delta_x\psi + 2\nabla_x\psi$. Using Lemma 4, the following equation for Schrödinger's momentum operator is obtained:

$$\frac{d}{dt}\langle \psi, x_j\psi \rangle = \frac{1}{m}\langle \psi, -i\hbar\nabla_j\psi \rangle.$$

The proof of this is analogue to the proof for Heisenberg's representation of the momentum operator when using Lemma 4. From the result of the proof, it follows that Schrödinger's representation of the momentum operator is in accordance with classical mechanics.

2.4 Spin

All quantum particles have a property called *spin*, which tells us what a “quantum particle looks like from different directions,” and is denoted by $\sigma \in \mathbb{N}_0 \cup \{1/2\}$. The existence of spin has been revealed in some experiments, for example the *Stern-Gerlach experiment*. In this experiment, silver atoms travel through an inhomogeneous magnetic field, such that they are deflected and have no orbital angular momentum. It had been expected that all atoms would be deflected down, and would struck on a detector screen. But, instead of a continuous distribution, there were discrete points of accumulation on the screen, which could be explained via the introduction of spin. A representation of this experiment is in the figure below.

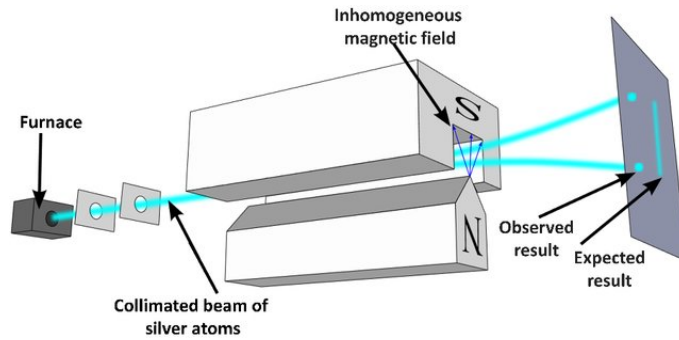


Figure 2: *Stern-Gerlach experiment setup*. Source: [Masi]

Bosons, for example *photons*, are particles with integer spin $\sigma \in \{0, 1, 2, \dots\}$. *Fermions* are the particles with spin $1/2$. Examples of such particles are electrons, protons and neutrons. Each quantum particle is either a boson or a fermion. To give an analogy for a more intuitive description for integer spin, playing cards are used. A particle having spin 0 can be compared to a dot, which looks the same from all directions. A particle of spin 1 can be depicted as an arrow and when turning it around a complete revolution, the particle looks the same, just like an ace of spades playing card (Figure 3). Particles of spin 2 can be compared to double-headed arrows: they look the same when turning it half a revolution round, like a queen of hearts playing card (Figure 4). [Hawking1988]

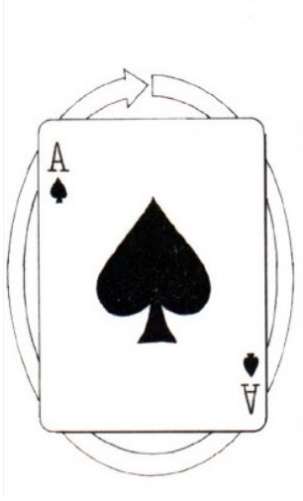


Figure 3: *An ace of spades playing card.* Source: [Hawking1988]



Figure 4: *A queen of hearts playing card.* Source: [Hawking1988]

Fermions, having spin $\sigma = 1/2$, need two revolutions to look the same, which cannot be compared with a real-world analogue. In practice, we will mostly deal with fermions.

2.5 Comparison of quantum mechanics with classical mechanics

Transforming a classical mechanical setting into a quantum mechanical setting is called *quantization*. In doing so, the quantum particles *should* also satisfy the laws of classical mechanics. However, this is generally not possible, since not all quantum mechanical properties have classical counterparts. For instance, spin, this property has no classical counterpart. Because e.g. spin cannot be quantized from something classical mechanical, the quantization of classical systems does not lead to an overall description of the quantum systems. In classical mechanics, the state space is in \mathbb{R}^d ; however, for quantum mechanics, this is $L^2(\mathbb{R}^d)$. Another difference deals with observables: in classical mechanics, these are real functions, whereas in quantum mechanics, these are self-adjoint operators. Also, there is a difference between the result of measuring an observable: in classical mechanics, this is deterministic, but in quantum mechanics, it is probabilistic. An example is position: in classical mechanics, this is known, and can be described in Cartesian coordinates. In quantum mechanics, the probability distribution $|\psi(\cdot, t)|^2$ is used to describe the probability of finding a particle at position x . [Gustafson and Sigal2011]

2.6 The uncertainty principle

In quantum mechanics, *Heisenberg's uncertainty principle* states that there is a limit to the precision of certain pairs of physical properties of a particle that can be known. By precision, we mean that if one wants to have a high-accurate measurement of one of the pair, the other

one has a low precision measurement. An example of this is the pair (x, p) . The Heisenberg uncertainty principle is formulated as follows:

Theorem 2. For $\psi \in L^2(\mathbb{R}^d)$, the refined uncertainty principle is given by

$$-\Delta_x \geq \frac{1}{4|x|^2}.$$

A proof of this can be found in [Gustafson and Sigal2011, Chapter 5]. The refined uncertainty principle is used as lower bound for the energy and can be used to show that molecules and atoms are *stable*, i.e. that the electrons do not collapse into the nucleus. In classical mechanics, atoms and molecules are seen as unstable. The stability of a quantum mechanical system is shown for the hydrogen atom in Chapter 3.

2.7 Spectrum and dynamics

An important observable is the energy of a system, for which the Schrödinger operator H is needed. In order to know more about the different energy values, the *spectrum* of H is needed. From the spectrum of H , the eigenvalues can be obtained, which are called the *bound-state energies*.

Definition 11. The spectrum of an operator A is

$$\sigma(A) := \{\lambda \in \mathbb{C} | A - \lambda \text{Id is not invertible}\}.$$

The spectrum can be divided into two parts: the *discrete spectrum*, $\sigma_d(A)$, and the *essential spectrum*, $\sigma_{ess}(A)$. The discrete spectrum contains the eigenvalues λ which are disjoint from the rest of $\sigma(A)$ around some neighbourhood of λ . The remainder of the spectrum is the essential spectrum.

Two important spectral theorems are the following ones:

Theorem 3. The spectrum of a self-adjoint operator is real.

Proof: See [Gustafson and Sigal2011, Chapter 23].

Theorem 4. For a continuous potential $V : \mathbb{R}^d \rightarrow \mathbb{R}$ with $V(x) \rightarrow 0$ as $|x| \rightarrow \infty$, the essential spectrum is given by $\sigma_{ess}(H) = [0, \infty)$ for $H = -\frac{\hbar^2}{2m}\Delta_x + \mathcal{V}$.

Proof: See [Gustafson and Sigal2011, Chapter 6].

The *ionization threshold* is given by the zero-energy level: above this threshold, the particle moves freely and is thus no longer localized. The ionization threshold and the energies below it are depicted in Figure 5 for the hydrogen atom.

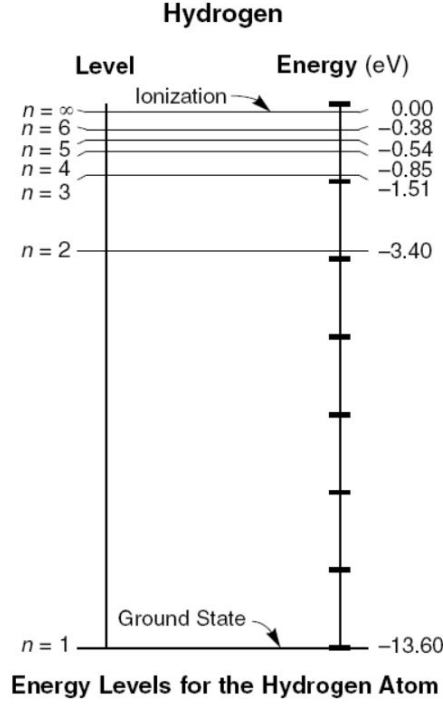


Figure 5: *Energy levels and ionization threshold for the hydrogen atom, in which each energy level corresponds to the energy of the n^{th} states.* Source: [Masi]

2.8 The many-particle system in \mathbb{R}^3

An example of quantization is the quantization of the *many-particle system*. Examples of many-particle systems are atoms or molecules, which interact with each other via *Coulomb forces*, which are the electrostatic forces between electrically charged particles. In a many-particle system, there are n particles, with masses m_1, \dots, m_n , classical positions $z = (z_1, \dots, z_n)$, and classical momenta $k = (k_1, \dots, k_n)$. The state of the classical system is given by (z, k) , and the dynamics are described by the classical *Hamiltonian function* $h(z, k)$ with potential $V_{\text{CM}}(z)$:

$$h(z, k) := \sum_{j=1}^n \frac{1}{2m_j} k_j^2 + V_{\text{CM}}(z),$$

where $V_{\text{CM}}(z)$ is given by

$$V_{\text{CM}}(z) := \frac{1}{2} \sum_{i \neq j}^n V_{ij}(z_i - z_j).$$

This system can be seen as the sum of two-body problems, where the interaction of each particle is only with one other particle. Furthermore, V_{ij} are individual potentials. For the quantized version of the many-particle system, we identify particle coordinates z_j with quantum particle coordinates x_j . The same can be done for momenta: p_j is the quantized version of momenta k_j , conform Definition 10. This way the classical Hamiltonian is quantized

2. INTRODUCTION TO QUANTUM MECHANICS

into the *quantum Hamiltonian*, H_{QM} , which is the Schrödinger operator with V_{QM} a general potential:

$$H_{\text{QM}}(x, p) := \sum_{j=1}^n \frac{1}{2m_j} |p_j|^2 + V_{\text{QM}}(x).$$

A general example of a many-particle system is a molecule consisting of N electrons with masses m and charges $-e$ and M nuclei of masses m_j and charges $Z_j e$, $j = 1, \dots, M$. The Schrödinger operator is then given by

$$H_{\text{QM}}(x, y, p, q) = \sum_{j=1}^N \frac{1}{2m} |p_j|^2 + \sum_{j=1}^M \frac{1}{2m_j} |q_j|^2 + V(x, y),$$

in which $x = (x_1, \dots, x_N) \in \mathbb{R}^{3N}$ are the electron coordinates and $y = (y_1, \dots, y_M) \in \mathbb{R}^{3M}$ are the nuclear coordinates. Also, $p_j = -i\hbar \partial_{x_j}$ is the momentum operator on the j -th electron and $q_j = -i\hbar \partial_{y_j}$ the momentum operator on the j -th nucleus. The potential $V(x, y)$ is defined by

$$V(x, y) := \frac{1}{2} \sum_{i \neq j}^N \frac{e^2}{|x_i - x_j|} - \sum_{i=N+1}^{N+M} \frac{e^2 Z_i}{|x_i - y_j|} + \frac{1}{2} \sum_{i \neq j}^M \frac{e^2 Z_i Z_j}{|y_i - y_j|}.$$

This potential consist of three parts. When reading from left to right, the terms are respectively the sum of Coulomb interaction potentials between the electrons internally, between the electrons and nuclei and between the nuclei internally. If $M = 1$, the system describes one atom. For a system with a single electron at position x , the *Coulomb potential* is given by $V(x) = -\frac{e^2}{|x|}$.

2.9 Summary

In this chapter, an overview of quantum mechanics has been given, with the Schrödinger equation (1) with the Schrödinger operator H as its most important tool. For the Schrödinger operator (4) with free motion, symmetry and self-adjointness have been proven. Observables have been discussed in the light of the two main representations. The spin property of quantum particles has been explained. We will mostly deal with fermions, which are the particles with half spin. By using Heisenberg's refined uncertainty principle, which gives a lower bound for the energy, stability of molecules and atoms can be shown. The spectrum of an operator gives us the bound-state energies of a quantum mechanical system. Lastly, the quantization of classical mechanical many-particle systems into quantum mechanical systems has been discussed. In Chapter 3, we will now study a specific many-particle system, namely the *hydrogen atom*.

3 The hydrogen atom

In the last section of the previous chapter, the many-particle system has been discussed. As was mentioned, an example of such a many-particle system is the hydrogen atom, which will be discussed in detail in this chapter. The hydrogen atom is the simplest quantum mechanical molecular model, since it only consists of a single proton and electron. The proton and electron interact with each other via *Coulomb forces*. In order to simplify the problem, we fix the proton of the nucleus in the origin, and make it infinitely heavy, such that in our model it does not move away from the origin. The electron moves around this proton due to Coulomb forces, which are described by the *external (Coulomb) potential* $V(x) = -\frac{e^2}{|x|}$, where $-e$ is the charge of the electron and $+e$ of the proton. This leads to the Schrödinger operator H_{hyd} , defined by

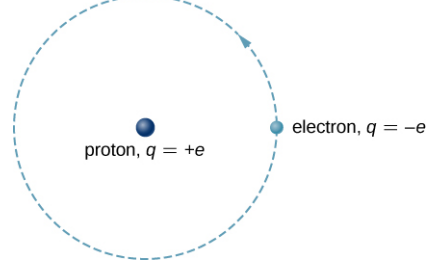


Figure 6: *Model of the hydrogen atom.* Source: [Urone2019]

$$H_{\text{hyd}} := -\frac{\hbar^2}{2m}\Delta_x - \frac{e^2}{|x|}. \quad (6)$$

To show the boundedness of this operator, the refined uncertainty principle from §2.6 is used, and we obtain the following inequalities:

$$\begin{aligned} H_{\text{hyd}} &= -\frac{\hbar^2}{2m}\Delta_x - \frac{e^2}{|x|} \\ &\geq \frac{\hbar^2}{8m|x|^2} - \frac{e^2}{|x|} \quad \left(\text{which has its minimum at } \frac{1}{|x|} = \frac{4me^2}{\hbar^2} \right) \\ &\geq -\frac{2me^4}{\hbar^2}. \end{aligned}$$

This result shows the energy of the hydrogen atom is bounded from below: therefore, the electron does not collapse into the nucleus and the atom is stable. The next step is to find possible energy values, for which we need the spectrum of H_{hyd} .

Theorem 5. *Assume that H_0 is a self-adjoint operator, and V is a symmetric operator satisfying $\|V\psi\| \leq a\|H_0\psi\| + b\|\psi\|$ for some $a < 1$ and $b \in \mathbb{R}$. Then the operator $H := H_0 + V$ with $D(H) = D(H_0)$ is self-adjoint.*

A proof of this can be found in [Gustafson and Sigal2011, Chapter 2]. The proof consists of two steps, first one has to prove that $(H + i\lambda)\psi = f$ has a solution. Next it must be shown that $\|V(H_0 + i\lambda)\| < 1$. Because the operator H_{hyd} can be written as $H_{\text{hyd}} = H_0 + V$, with H_0 self-adjoint and V symmetric, it follows from Theorem 5 that H_{hyd} is self-adjoint. Also, since $V : \mathbb{R}^d \rightarrow \mathbb{R}$ is continuous with $V(x) \rightarrow 0$ as $|x| \rightarrow \infty$, it follows that $\sigma_{\text{ess}}(H_{\text{hyd}}) = [0, \infty)$ by Theorem 4.

The goal now is to find the eigenfunctions (the *bound-states*) and eigenvalues (the *bound-state energies*) of H_{hyd} , by solving the eigenvalue problem

$$H_{\text{hyd}}\psi_n^*(\cdot, t) = E_n\psi_n^*(\cdot, t) \text{ for fixed } t, \quad (7)$$

3. THE HYDROGEN ATOM

in which $\psi_n^*(\cdot, t)$ are the eigenfunctions for a fixed t and therefore stationary. Note that (7) is also known as the *stationary Schrödinger equation*, which follows from the original Schrödinger equation (1) by separation of the variables in space and time. A proof of the separation of variables can be found in [Parris2019]. In this proof, separation of variables is interpreted as the decomposition of the original, multivariate space into the direct product of the different in spaces. Note that it is quite remarkable that these eigenvalues and eigenfunctions can be found explicitly, since there are only a few other models for which the eigenvalue problem (7) can be solved explicitly, e.g. the harmonic oscillator. [Suryanarayana et al.2013]

For the hydrogen atom, we have $x \in \mathbb{R}^3$. Due to the fact that the Coulomb potential $V(x)$ can be written as a function of $|x|$, it is easier to move to spherical coordinates (r, θ, ϕ) with $r = |x|, x = (x, y, z)^T$:

$$x = r \sin(\theta) \cos(\phi) \quad y = r \sin(\theta) \sin(\phi) \quad z = r \cos(\theta),$$

with polar and azimuthal angles $0 \leq \theta < \pi$, respectively $0 \leq \phi < 2\pi$. For spherical coordinates, the Laplacian can be written as

$$\Delta_x = \frac{1}{r^2} \frac{\partial}{\partial r} \left(r^2 \frac{\partial}{\partial r} \right) + \frac{1}{r^2 \sin(\theta)} \frac{\partial}{\partial \theta} \left(\sin(\theta) \frac{\partial}{\partial \theta} \right) + \frac{1}{r^2 \sin^2(\theta)} \frac{\partial^2}{\partial \phi^2}.$$

This can be split into two parts

$$\Delta_x = \Delta_r + \frac{1}{r^2} \Delta_\Omega, \quad (8)$$

in which Δ_r is the *radial Laplacian*, defined as

$$\Delta_r := \frac{1}{r^2} \frac{\partial}{\partial r} \left(r^2 \frac{\partial}{\partial r} \right), \quad (9)$$

and Δ_Ω is the *Laplace-Beltrami operator*, defined as

$$\Delta_\Omega := \frac{1}{\sin(\theta)} \frac{\partial}{\partial \theta} \left(\sin(\theta) \frac{\partial}{\partial \theta} \right) + \frac{1}{\sin^2(\theta)} \frac{\partial^2}{\partial \phi^2}. \quad (10)$$

Because H_{hyd} can be separated in its variables, we obtain for the wave functions $\psi_n^*(r, \theta, \phi)$

$$\psi_n^*(r, \theta, \phi) := R_{nl}(r) Y_l^k(\theta, \phi), \quad n \in \{1, \dots, N_p\}, \quad (11)$$

in which N_p depends on the number of orbitals, also we have $l \in \{-n, \dots, n\}$ and $k \in \{-l, \dots, l\}$. Note that the parameter t has been dropped. The principal quantum number is denoted by n , and describes the size of the orbital and the energy an electron has in this orbital. The number of the orbital, l , describe the shape of the orbital. The magnetic quantum number is denoted by k , and describes the energy distribution within an orbital.

Definition 12. $R_{nl}(r)$ are the radial wave functions and Y_l^k are spherical harmonics, defined as

$$Y_l^k(\theta, \phi) := c_{lk} P_l^{|k|}(\cos(\theta)) e^{ik\phi},$$

where $l \in \mathbb{N}_0$, $k \in \{-l, -l+1, \dots, l-1, l\}$, $n \in \{l+1, l+2, \dots\}$, $c_{lk} \in \mathbb{R}$ are constants, $P_l^{|k|}$ is an associated Legendre function, defined as

$$P_l^{|k|}(u) := \frac{(1-u^2)^{|k|/2}}{(2^l)(l!)^2} \left(\frac{d}{du} \right)^{l+k} \left((u^2-1)^l \right).$$

3. THE HYDROGEN ATOM

In Y_l^k , $u = \cos(\theta)$. All the associated Legendre functions satisfy the *associated Legendre differential equation*

$$(1-u^2)\frac{d^2}{du^2}P_l^k(u) - 2u\frac{d}{du}P_l^k(u) + \left[l(l+1) - \frac{k^2}{1-u^2}\right]P_l^k(u) = 0. \quad (12)$$

For $u = \cos(\theta)$, this can be written as

$$c_{lk}e^{ik\phi}\frac{1}{\sin(\theta)}\frac{\partial}{\partial\theta}\left(\sin(\theta)\frac{\partial}{\partial\theta}P_l^k(u)\right) + \left(l(l+1) + \frac{1}{\sin^2(\theta)}\frac{\partial^2}{\partial\phi^2}\right)P_l^k(u)c_{lk}e^{ik\phi} = 0. \quad (13)$$

A proof of (13) can be found in [2011AssociatedFunction] in which the *Legendre function* P_l^k is used, given by the equation $P_l^k(u) = \frac{(1-u^2)^{k/2}}{2^l l!} \left(\frac{d}{du}\right)^{l+k} (u^2-1)^l$. This gives the following relation for Δ_Ω :

$$-\Delta_\Omega Y_l^k = l(l+1)Y_l^k. \quad (14)$$

Proof: See [Boyle2010]. Using this information on the Laplace-Beltrami operator and substitution of $\psi_n^*(r, \theta, \phi) = R_{nl}(r)Y_l^k(\theta, \phi)$ into (7), we obtain the following Lemma:

Lemma 5.

$$\left(\frac{\hbar^2}{2m}\left[-\Delta_r + \frac{l(l+1)}{r^2}\right] - \frac{e^2}{r}\right)R_{nl}(r) = E_n R_{nl}(r). \quad (15)$$

Proof: This is true due to the following equivalences:

$$\begin{aligned} H\psi_n^*(r, \theta, \phi) &= E_n\psi_n^*(r, \theta, \phi) && \Longleftrightarrow \\ HR_{nl}(r)Y_l^k(\theta, \phi) &= E_n R_{nl}(r)Y_l^k(\theta, \phi) && \Longleftrightarrow \\ \left(-\frac{\hbar^2}{2m}\Delta_{\mathbf{x}} - \frac{e^2}{r}\right)R_{nl}(r)Y_l^k(\theta, \phi) &= E_n R_{nl}(r)Y_l^k(\theta, \phi) && \Longleftrightarrow \\ \left(\frac{\hbar^2}{2m}\left[-\Delta_r - \frac{1}{r^2}\Delta_\Omega\right] - \frac{e^2}{r}\right)R_{nl}(r)Y_l^k(\theta, \phi) &= E_n R_{nl}(r)Y_l^k(\theta, \phi) && \Longleftrightarrow \\ \left(\frac{\hbar^2}{2m}\left[-\Delta_r + \frac{l(l+1)}{r^2}\right] - \frac{e^2}{r}\right)R_{nl}(r)Y_l^k(\theta, \phi) &= E_n R_{nl}(r)Y_l^k(\theta, \phi). && \square \end{aligned}$$

Ansatz 1. The radial wave functions R_{nl} are defined as

$$R_{nl}(\rho) := \rho^l e^{-\rho/2} F_{nl}(\rho), \quad (16)$$

in which $F_{nl}(\rho)$ are polynomials of degree l depending on $\rho(r)$, with $\rho(r)$ defined as

$$\rho(r) := \frac{n\hbar^2}{2me^2}r.$$

Note that $\rho(r)$ depends on n ; however, for readability we will write $\rho_n(r) = \rho(r)$.

Theorem 6. *The eigenvalues of eigenvalue problem (7) are given by*

$$E_n = - \left(\frac{me^4}{2\hbar^2} \right) \frac{1}{n^2}, \quad n \in \{l+1, l+2, \dots, N_p\}, \quad (17)$$

and that the many-particle system only has solutions for $\psi^*(\cdot, t) \in L^2(\mathbb{R}^3)$ if

$$n = \frac{e^2}{\hbar} \sqrt{\frac{-m}{2E}}. \quad (18)$$

The proof of this can be found in the following section. Note that the bound-state energies are negative.

3.1 Proof of Theorem 6

In order to prove Theorem 6, we first write $F_{nl}(\rho)$ as a finite power series, as it is a polynomial. Secondly, coordinate transformations are used. Lastly, (16), with $F_{nl}(\rho)$ written as a power series, is substituted in (15).

Writing F_{nl} as a power series

Since F_{nl} is a polynomial, it can be expressed in the following power series, where l denotes the degree of the polynomial:

$$F_{nl}(\rho) = \sum_{k=-l}^l c_k \rho^k, \quad c_k \in \mathbb{C}. \quad (19)$$

For the first and second derivative, we get

$$\frac{dF_{nl}}{d\rho}(\rho) = \sum_{k=-l}^l c_k k \rho^{k-1} \quad \frac{d^2 F_{nl}}{d\rho^2}(\rho) = \sum_{k=-l}^l c_k k(k-1) \rho^{k-2}. \quad (20)$$

Coordinate transformations

It has been given that $\rho = n\hbar^2 r / (2me^2)$; this is equivalent to

$$r = a\rho \quad \text{with} \quad a := \frac{2me^2}{n\hbar^2}.$$

We then get

$$\frac{\partial^j}{\partial r^j} = a^j \frac{\partial^j}{\partial \rho^j} \quad \forall j \in \mathbb{N}.$$

Using this, (15) can be expressed in terms of ρ as

$$\left(\frac{\hbar^2}{2m} \left[-a^2 \frac{\partial^2}{\partial \rho^2} - \frac{2}{\rho} \frac{\partial}{\partial \rho} + \frac{l(l+1)}{a^2 \rho^2} \right] - \frac{e^2}{a\rho} \right) R_{nl}(\rho) Y_l^k(\theta, \phi) = E_n R_{nl}(\rho) Y_l^k(\theta, \phi) \quad (21)$$

Since the term $Y_l^k(\theta, \phi)$ in (11) and (21) is independent of ρ , it is not taken into account when calculating the partial derivatives of $\psi_n^* = \psi_n^*(\rho, \theta, \phi)$ with respect to ρ .

3. THE HYDROGEN ATOM

Using the product rule and (16), the first partial derivative of ψ_n^* is

$$\frac{\partial \psi_n^*}{\partial \rho}(\rho, \theta, \phi) = \frac{d}{d\rho} R_{nl}(\rho) Y_l^k(\theta, \phi) = \left(\left(\frac{l}{\rho} - \frac{1}{2} \right) F_{nl}(\rho) + \frac{d}{d\rho} F_{nl}(\rho) \right) \rho^l e^{-\rho/2} Y_l^k(\theta, \phi), \quad (22)$$

and the second one is

$$\begin{aligned} \frac{\partial^2 \psi_n^*}{\partial \rho^2}(\rho, \theta, \phi) &= \frac{d^2}{d\rho^2} R_{nl}(\rho) Y_l^k(\theta, \phi) = \left(\left(\frac{l(l-1)}{\rho^2} - \frac{l}{\rho} + \frac{1}{4} \right) F_{nl}(\rho) + \right. \\ &\quad \left. \left(\frac{2l}{\rho} - 1 \right) \frac{d}{d\rho} F_{nl}(\rho) + \frac{d^2}{d\rho^2} F_{nl}(\rho) \right) \rho^l e^{-\rho/2} Y_l^k(\theta, \phi). \end{aligned} \quad (23)$$

Substitution in (21)

Since we now have expressions for the first two partial derivatives of ψ_n^* w.r.t. ρ , these can be used in (21). Also, it is known that the terms ρ^l , $e^{-\rho/2}$ and $Y_l^k(\theta, \phi)$ are not equal to zero for $\rho \neq 0$: using this as well, we get

$$\begin{aligned} \frac{\hbar^2}{2m} \left[-a^2 \left(\left(\frac{l(l-1)}{\rho^2} - \frac{l}{\rho} + \frac{1}{4} \right) F_{nl}(\rho) + \left(\frac{2l}{\rho} - 1 \right) \frac{d}{d\rho} F_{nl}(\rho) + \frac{d^2}{d\rho^2} F_{nl}(\rho) \right) \right. \\ \left. - \frac{2}{\rho} \left(\left(\frac{l}{\rho} - \frac{1}{2} \right) F_{nl}(\rho) + \frac{d}{d\rho} F_{nl}(\rho) \right) + \frac{l(l+1)}{a^2 \rho^2} F_{nl}(\rho) \right] - \left[\frac{e^2}{a\rho} F_{nl}(\rho) + E_n F_{nl}(\rho) \right] = 0. \end{aligned}$$

For $F_{nl}(\rho)$ and its derivatives, the power series from (19) and (20) are substituted into the equation above. Collecting the equal terms, we obtain

$$\begin{aligned} \sum_{k=-l}^l c_k \rho^{k-2} \left(\frac{-a^2 \hbar^2}{2m} \left((l^2 - 3l) + \frac{l^2 + l}{a^2} \right) \right) + \sum_{k=-l}^l c_k \rho^{k-1} \left(\frac{-a^2 \hbar^2}{2m} (-l+1) - \frac{e^2}{a} \right) + \\ \sum_{k=-l}^l c_k \rho^k \left(-E_n - \frac{a^2 \hbar^2}{8m} \right) + \sum_{k=-l}^l c_k k \rho^{k-2} \left(\frac{a^2 \hbar^2}{m} (l-1) \right) + \\ \sum_{k=-l}^l c_k k \rho^{k-1} \left(\frac{-a^2 \hbar^2}{2m} \right) + \sum_{k=-l}^l c_k k(k-1) \rho^{k-2} \left(\frac{-a^2 \hbar^2}{2m} \right) = 0. \end{aligned}$$

Now we shift the sum indices in order to factor out ρ^k :

$$\begin{aligned} \sum_{k=-l-2}^{l-2} c_{k+2} \rho^k \left(\frac{-a^2 \hbar^2}{2m} \left((l^2 - 3l) + \frac{l^2 + l}{a^2} \right) \right) + \sum_{k=-l-1}^{l-1} c_{k+1} \rho^k \left(\frac{-a^2 \hbar^2}{2m} (-l+1) - \frac{e^2}{a} \right) + \\ \sum_{k=-l}^l c_k \rho^k \left(-E_n - \frac{a^2 \hbar^2}{8m} \right) + \sum_{k=-l-2}^{l-2} c_{k+2} (k+2) \rho^k \left(\frac{a^2 \hbar^2}{m} (l-1) \right) + \\ \sum_{k=-l-1}^{l-1} c_{k+1} (k+1) \rho^k \left(\frac{-a^2 \hbar^2}{2m} \right) + \sum_{k=-l-2}^{l-2} c_{k+2} (k+2)(k+1) \rho^k \left(\frac{-a^2 \hbar^2}{2m} \right) = 0. \end{aligned}$$

3. THE HYDROGEN ATOM

For $k \in \{-l, 1, 2, \dots, l-2\}$ the following relation is obtained for the ρ^k -term:

$$c_{k+2} \left(\frac{-a^2 \hbar^2}{2m} \left((l^2 - 3l) + \frac{l^2 + l}{a^2} \right) + (k+2) \left(\frac{-a^2 \hbar^2}{m} (l-1) \right) + (k+2)(k+1) \left(\frac{-a^2 \hbar^2}{2m} \right) \right) + c_{k+1} \left(\frac{-a^2 \hbar^2}{2m} (-l+1) - \frac{e^2}{a} + (k+1) \frac{a^2 \hbar^2}{2m} \right) + c_k \left(-E_n - \frac{a^2 \hbar^2}{8m} \right) = 0.$$

For $k \in \{l-1, l\}$ we get fewer terms because $c_{l+1} = c_{l+2} = 0$, since the degree of F_{nl} is l : so for $k = l$, this leads to

$$c_{l+2} \frac{-a^2 \hbar^2}{2m} \left(\left(4 + \frac{1}{a^2} \right) k^2 + \left(2 + \frac{1}{a^2} \right) k - 2 \right) + c_{l+1} \left(\frac{-a^2 \hbar^2}{2m} - \frac{e^2}{a} \right) = \left(E_n + \frac{-a^2 \hbar^2}{8m} \right) c_l.$$

As was noted before, this power series has to terminate somewhere. Using $c_{l+1} = c_{l+2} = 0$, gives us the equation

$$0 = \left(\frac{a^2 \hbar^2}{8me} + E_n \right) c_l \implies E_n = -\frac{a^2 \hbar^2}{8me}.$$

Now, replacing $a = \frac{n\hbar^2}{2me^2}$, we obtain the eigenvalues

$$E_n = -\frac{\hbar^2}{8m \left(\frac{n\hbar^2}{2me^2} \right)^2} = -\frac{me^4}{2n^2 \hbar^2} = -\left(\frac{me^4}{2\hbar^2} \right) \frac{1}{n^2},$$

and the eigenvalue problem (15) has solutions $\psi \in L^2(\mathbb{R}^3)$ for the restriction

$$n = \frac{e^2}{\hbar} \sqrt{\frac{-m}{2E_n}} \in \{l+1, l+2, \dots, N_p\}.$$

3.2 Example of a radial wave function

The radial wave functions $R_{nl}(r)$ can be determined for certain pairs of (n, l) , e.g. $(n, l) = (1, 0)$. The wave functions are normalized and therefore should satisfy

$$1 = \int_{\mathbb{R}^3} |\psi(x)|^2 d^3x. \quad (24)$$

For the spherical wave function $\psi_n^*(\rho, \theta, \phi)$, this transforms into

$$1 = \int_0^{2\pi} \int_0^\pi \int_0^\infty |R_{nl}(r) Y_l^k(\theta, \phi)|^2 r^2 \sin \phi dr d\theta d\phi. \quad (25)$$

However, $Y_l^k(\theta, \psi)$ has the following property: [Jeffreys1955]

$$\int_0^{2\pi} \int_0^\pi |Y_l^k(\theta, \phi)|^2 \sin \phi d\theta d\phi = 1,$$

and therefore we have the following restriction for $R_{nl}(r)$:

$$\int_0^\infty |R_{nl}(r)|^2 r^2 dr = 1. \quad (26)$$

3. THE HYDROGEN ATOM

Following (16) and using $F_{10}(r) = c_0 \rho^0 = c_0$, R_{10} can be expressed as

$$R_{10}(r) = c_0 \exp(-\rho/2), \quad \text{with } \rho = \frac{\hbar^2}{2me^2} r,$$

which gives us

$$c_0^2 \int_0^\infty r^2 \exp\left(-\frac{\hbar^2}{2me^2} r\right) dr = 1. \quad (27)$$

Now, the following relation is used:

$$\int_0^\infty r^n \exp(-\alpha r) dr = \frac{n!}{\alpha^{n+1}}.$$

This results in

$$c_0^2 \int_0^\infty r^2 \exp\left(-\frac{\hbar^2}{2me^2} r\right) dr = 2c_0^2 \cdot \left(\frac{\hbar^2}{2me^2}\right)^{-3} \stackrel{!}{=} 1.$$

For c_0 , we then obtain the value

$$c_0 = \frac{\hbar^3}{4m^{3/2}e^3},$$

and for the wave function R_{10} , we have that

$$R_{10}(r) = \frac{\hbar^3}{4m^{3/2}e^3} e^{-\frac{\hbar^2}{4me^2} r}. \quad (28)$$

3.3 Energy states

The *ground state* is the state in which the system has its lowest energy. Any state having higher energy than the ground state is called an *excited state*. In a quantum system, the *degeneracy* of the energy levels E_n is the number of different states giving the same energy value. For the hydrogen atom, the degeneracy of the energy levels is

$$\sum_{l=0}^{n-1} (2l+1) = 2 \sum_{l=0}^{n-1} l + \sum_{l=0}^{n-1} 1 = 2 \binom{n}{2} + n = 2 \frac{(n-1)n}{2 \cdot 1} + \frac{2n}{2} = \frac{2n^2 - 2n + 2n}{2} = n^2.$$

This is due to the fact that for a given l , there are $2l+1$ different values allowed for k , since $k \in \{-l, -l+1, \dots, 0, \dots, l-1, l\}$. Furthermore, for a given n , there are n different values allowed. Each orbital has a different shape; the first ones are the **s**, **p**, **d** and **f** orbitals. For the hydrogen-like atomic orbitals of different values of (n, l) , see the following image in which **s** means $l=0$, **p**: $l=1$, **d**: $l=2$ and **f**: $l=3$.

3. THE HYDROGEN ATOM

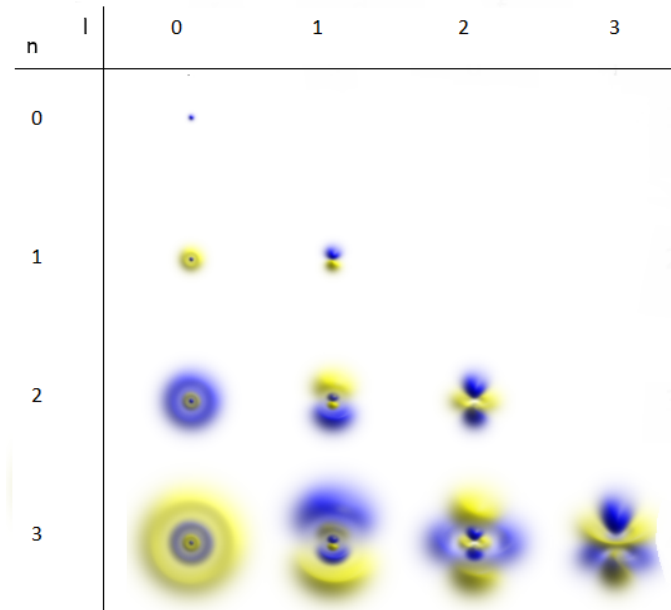


Figure 7: *Electron probability densities for different values of (n, l) for the hydrogen atom. The blue colour corresponds to the regions where the wave function is positive and yellow for negative. Sources: [Zunger2018, Halpern2019]*

The value for E_n in (17) is also in line with the empirical formula found by Balmer:

$$\Delta E_{i_f} := E_{n_f} - E_{n_i} = R \left(\frac{1}{n_f^2} - \frac{1}{n_i^2} \right),$$

where $R := -me^4\hbar^{-2}/2$, n_i is the initial state and n_f the final state of a *radiation process*, the process in which an unstable nucleus loses energy via emission of radiation. The set of spectral lines for a given final state n_f are usually dense. For the hydrogen atom, these states are given specific names: the initial states having final state $n_f = 1$, for example, are called the *Lyman series*, the ones having final state $n_f = 2$ the *Balmer series* and the ones with final state $n_f = 3$ the *Paschen series*. The Balmer series is of importance in astronomy, since many of these spectral lines are in visible light. In Figure 8, an overview of different levels and their names is given for the hydrogen atom.

3. THE HYDROGEN ATOM

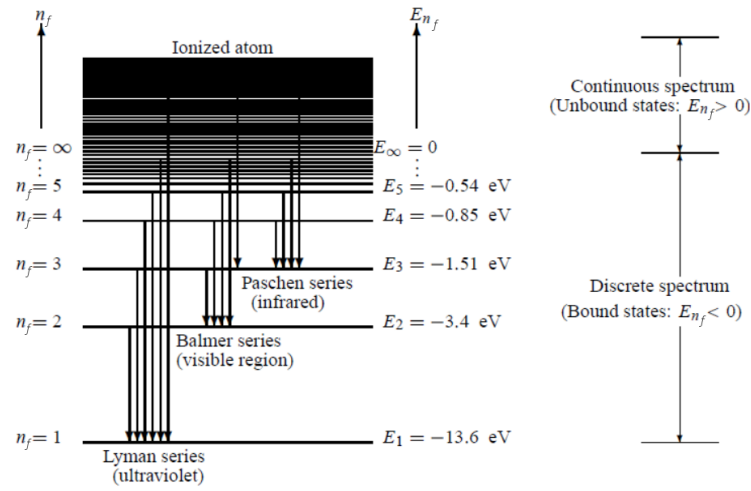


Figure 8: *Energy levels of the hydrogen atom with the corresponding names, with E the energy levels. For $n \rightarrow \infty$ the energy converges to 0, above this the hydrogen atom is ionized. Source: [Igmur2017]*

4 Electronic structure theory of many-electron systems

In this section, we will look at the electronic structure of many-electron systems, like molecules and atoms. Solving eigenvalue systems to find wave functions is complicated. In the previous chapter, it has been shown that for a small number of simple cases, like the hydrogen atom, the eigenvalue problem (7) can be solved analytically. When systems become more complex, like large atoms or molecules, this cannot be done: so for these cases, numerical approximating methods are needed. The methods discussed in this chapter are the *Born-Oppenheimer approximation* and the *Hartree-Fock method*. The Born-Oppenheimer approximation decouples the Hamiltonian in an electronic and nuclear part. However, these methods become less accurate and take more computational time when it comes to larger systems. Therefore, a third method is discussed, called *Density Functional Theory* (DFT). This method is popular, because it has a good balance [Erhart2016] between accuracy and computational costs, which enable calculations for large systems.

For systems involving multiple electrons and nuclei, there is an interaction between electrons and nuclei. The Schrödinger operator for a molecule in general is given by

$$H_{\text{mol}} := T_{\text{n}} + T_{\text{e}} + V_{\text{e-n}} + V_{\text{n-n}} + V_{\text{e-e}}, \text{ where} \quad (29)$$

$$\begin{aligned} T_{\text{n}} &:= \sum_{\alpha=1}^{N_{\alpha}} \frac{-\hbar^2}{2M_{\alpha}} \Delta_{\mathbf{R}_{\alpha}} \\ T_{\text{e}} &:= \sum_{i=1}^{N_{\text{e}}} \frac{-\hbar^2}{2m} \Delta_{\mathbf{x}_i} \\ V_{\text{e-n}} &:= - \sum_{\alpha=1}^{N_{\alpha}} \sum_{i=1}^{N_{\text{e}}} \frac{Z_{\alpha} e^2}{|\mathbf{x}_i - \mathbf{R}_{\alpha}|} \\ V_{\text{n-n}} &:= \sum_{\alpha > \beta} \frac{Z_{\alpha} Z_{\beta} e^2}{|\mathbf{R}_{\alpha} - \mathbf{R}_{\beta}|} \\ V_{\text{e-e}} &:= \sum_{i > j} \frac{e^2}{|\mathbf{x}_i - \mathbf{x}_j|}, \end{aligned}$$

$\mathbf{R} = (\mathbf{R}_1, \dots, \mathbf{R}_{N_{\alpha}}) \in \mathbb{R}^{3N_{\alpha}}$ denotes the coordinates of the nuclei, with N_{α} the number of nuclei. Furthermore, $\mathbf{x} = (\mathbf{x}_1, \dots, \mathbf{x}_{N_{\text{e}}}) \in \mathbb{R}^{3N_{\text{e}}}$ denotes the coordinates of the electrons, where N_{e} is the number of electrons. Z_{α} is the *atomic number*, which is the amount of protons in the α -th nucleus. The mass of a nucleus α is given by M_{α} , and the mass of each electron is m . Next, T_{n} and T_{e} are the sum of all kinetic energy operators for the nuclei respectively the electrons, and $V_{\text{e-n}}$, $V_{\text{n-n}}$ and $V_{\text{e-e}}$ are the operators for respectively the electron-nucleus, nucleus-nucleus and electron-electron interactions. For the latter two, the potential energy comes from Coulomb repulsions.

4.1 The Born-Oppenheimer approximation

For the *Born-Oppenheimer approximation*³, it is assumed that the electronic and nuclear potentials can be separated in the Hamiltonian, using the fact that the nuclei are much heavier than the electrons, with $\frac{m}{M_\alpha} \approx 10^{-3}$; therefore, the electrons adjust to the motion of the nuclei, and the nuclei can thus be seen as fixed points. This way, we can split the Schrödinger operator (29) into two parts: the electronic part H_{el} and the nuclear part H_{n} . The mixed potential $V_{\text{e-n}}$ makes this separation hard, since it does not specifically belong to the electronic part, nor to the nuclear part. The associated eigenvalue problem reads

$$H_{\text{mol}}\psi_k^* = E_k\psi_k^*, \quad \text{with } H_{\text{mol}} = H_{\text{el}} + H_{\text{n}}, \quad (30)$$

where ψ_k^* is the stationary wave function and H_{el} and H_{n} are defined by

$$H_{\text{el}} := T_{\text{e}} + V_{\text{e-e}} + V_{\text{e-n}}, \quad H_{\text{n}} := T_{\text{n}} + V_{\text{n-n}}.$$

The operators H_{el} and H_{n} commute with each other. Because of this, both E_{el} and E_{n} have their own IVP. We can use separation of variables for the stationary wave functions [Parris2019] $\psi_k^*(\mathbf{x}, \mathbf{R})$ resulting in

$$\psi_k^*(\mathbf{x}, \mathbf{R}) = \phi_k(\mathbf{x})\chi_k(\mathbf{R}), \quad (31)$$

where $\phi_k(\mathbf{x})$ denotes the *electronic wave function* and $\chi_k(\mathbf{R})$ the *nuclear wave function*. For the eigenvalue problem in (30), we obtain

$$\begin{aligned} H_{\text{mol}}\psi_k^*(\mathbf{x}, \mathbf{R}) &= (H_{\text{el}} + H_{\text{n}}) \phi_k(\mathbf{x})\chi_k(\mathbf{R}) = H_{\text{el}}\phi_k(\mathbf{x})\chi_k(\mathbf{R}) + H_{\text{n}}\chi_k(\mathbf{R})\phi_k(\mathbf{x}) \\ &= (E_{\text{el},k} + E_{\text{n},k}) \phi_k(\mathbf{x})\chi_k(\mathbf{R}) \\ &\stackrel{!}{=} E_k\psi_k^*(\mathbf{x}, \mathbf{R}) \\ \implies H_{\text{el}}\phi_k &= E_{\text{el},k}\phi_k, \quad H_{\text{n}}\chi_k = E_{\text{n},k}\chi_k. \end{aligned}$$

Since the electrons adjust to the motion of the nuclei, due to the fact that nuclei are much more heavier than electrons, we can fix \mathbf{R} . So for $V_{\text{e-n}}(\mathbf{x}, \mathbf{R})$ is written as $V_{\text{e-n}}(\mathbf{x}; \mathbf{R})$, because $V_{\text{e-n}}$ depends on \mathbf{R} parametrically. Because of this, we write $\phi(\mathbf{x}; \mathbf{R})$ instead of $\phi(\mathbf{x}, \mathbf{R})$. Using this for H_{el} and H_{n} , we have

$$\begin{aligned} H_{\text{el}}(\mathbf{x}; \mathbf{R}) &= T_{\text{e}}(\mathbf{x}) + V_{\text{e-e}}(\mathbf{x}) + V_{\text{e-n}}(\mathbf{x}; \mathbf{R}) \\ H_{\text{n}}(\mathbf{x}) &= T_{\text{n}}(\mathbf{R}) + V_{\text{n-n}}(\mathbf{R}) + E_{\text{el}}(\mathbf{x}). \end{aligned}$$

$E_{\text{el},k}$ is obtained from solving the electronic eigenvalue problem for $k \in \{1, \dots, N_{\text{e}}\}$:

$$H_{\text{el}}\phi_k(\mathbf{x}; \mathbf{R}) = E_{\text{el},k}(\mathbf{R})\phi_k(\mathbf{x}; \mathbf{R}). \quad (32)$$

When solving for each electronic state k

$$(T_{\text{n}}(\mathbf{R}) + V_{\text{n-n}}(\mathbf{R}) + E_{\text{el}}(\mathbf{R})) \chi_j(\mathbf{R}) = E_{\text{n},j}(\mathbf{R})\chi_j(\mathbf{R}), \quad \text{with } E_{\text{n}}(\mathbf{R}) = \sum_{j=0}^{N_{\alpha}} E_{\text{n},j}(\mathbf{R}),$$

³This approximation was proposed by Max Born and Julius Robert Oppenheimer in 1927, and is still essential in quantum mechanics.

the nuclear eigenvalues $E_{n,j}(\mathbf{R})$ are obtained. Note that

$$E_{\text{eff}}(\mathbf{R}) := V_{n-n}(\mathbf{R}) + E_{\text{el}}(\mathbf{R})$$

is also called the *effective potential* or *potential energy surface* for each electronic state.

The advantage of this method is that the original problem is reduced from $3N_e + 3N_\alpha$ dimensions to only $3N_e$ dimensions. However, one should also find solutions to (32). A method for this, will be discussed in the next section.

4.2 The Hartree-Fock method

For the Born-Oppenheimer approximation, there are still N_e eigenvalue problems to solve. However, it could be simplified when we would treat the electrons as non-interacting single particles. In order to approximate (32) by a non-interacting single particle approximation, we use the *adapted electronic Hamiltonian*:

$$H_{\text{el}}^* := \sum_{i=1}^{N_e} h_i \quad \text{with} \quad h_i := \frac{-\hbar^2}{2m} \Delta_{\mathbf{x}_i} - \sum_{\alpha=1}^{N_\alpha} \frac{Z_\alpha e^2}{|\mathbf{x}_i - \mathbf{R}_\alpha|},$$

which commute with each other:

$$\forall i, j \in \{1, \dots, N_e\} : [h_i, h_j] = 0.$$

Electrons are fermions, and should satisfy particle exchange: this is due to *Pauli's exclusion principle*, stating that two or more identical fermions (in this case the electrons) cannot occupy the same quantum state within a quantum system simultaneously. Therefore, $\phi(\mathbf{x}; \mathbf{R})$ should be *fermionic*, meaning anti-symmetric with respect to the exchange of two identical electrons. [Gustafson and Sigal2011] From now on, we will drop the \mathbf{R} in $\phi(\mathbf{x}; \mathbf{R})$. When looking at the whole system of electrons, we cannot write $\phi(\mathbf{x})$ as a *Hartree product*, which is given by

$$\phi(\mathbf{x}_1, \dots, \mathbf{x}_{N_e}) = \phi_1(\mathbf{x}_1) \dots \phi_{N_e}(\mathbf{x}_{N_e}),$$

with ϕ_i as in (32), since it would not be fermionic. The labelling of the states should not matter either; and therefore, there should be permutation operators \mathbf{P}_{ij} such that the following holds:

$$\mathbf{P}_{ij} \phi(\mathbf{x}_1, \dots, \mathbf{x}_i, \dots, \mathbf{x}_j, \dots, \mathbf{x}_{N_e}) = \phi(\mathbf{x}_1, \dots, \mathbf{x}_j, \dots, \mathbf{x}_i, \dots, \mathbf{x}_{N_e}). \text{ for all } i, j \in \{1, \dots, N_e\}$$

Due to fermionicity of $\phi(\mathbf{x})$, $\mathbf{P}_{ij} = -\text{Id}$, and we have that

$$\phi(\mathbf{x}_1, \dots, \mathbf{x}_i, \dots, \mathbf{x}_j, \dots, \mathbf{x}_{N_e}) = -\phi(\mathbf{x}_1, \dots, \mathbf{x}_j, \dots, \mathbf{x}_i, \dots, \mathbf{x}_{N_e}).$$

In general for many-body systems, the fermionicity can be taken into account when taking a specific linear combination of Hartree products. We now come at the Hartree-Fock⁴ (HF) method. An expression satisfying the fermionicity of the wave function, is the *Slater determinant*. For the HF method, the following Ansatz has been made:

⁴The Hartree-Fock method is a method for finding the best possible single-particle wave functions. This method was first published by Douglas Hartree, and improved by Vladimir Fock two years later.

Ansatz 2. The wave function is given by a single Slater determinant.

$$\phi(\mathbf{x}) := \frac{1}{\sqrt{N_e!}} \begin{vmatrix} \phi_1(\mathbf{x}_1) & \phi_2(\mathbf{x}_1) & \cdots & \phi_{N_e}(\mathbf{x}_1) \\ \phi_1(\mathbf{x}_2) & \phi_2(\mathbf{x}_2) & \cdots & \phi_{N_e}(\mathbf{x}_2) \\ \vdots & \vdots & \ddots & \vdots \\ \phi_1(\mathbf{x}_{N_e}) & \phi_2(\mathbf{x}_{N_e}) & \cdots & \phi_{N_e}(\mathbf{x}_{N_e}) \end{vmatrix}. \quad (33)$$

In (33), the problem remains how to find $\phi_i(\mathbf{x}_j)$, if one has no independent electrons. The tool for finding this $\phi_i(\mathbf{x}_j)$, is *variation*. The *variational principle* states that any trial wave function $\tilde{\phi}(\mathbf{x}_1, \dots, \mathbf{x}_{N_e})$ will give an estimated energy $\tilde{E}_{\text{est}} \geq E_0$, in which E_0 is the true, minimal, *ground state energy* when solving the exact Schödinger equation. The eigenvalue problem electronic Hamiltonian (32) can be written as

$$H_{\text{el}}^* \phi_k = E_{\text{el},k} \phi_k \quad (34)$$

$$\langle \phi_k, H_{\text{el}}^* \phi_k \rangle = \langle \phi_k, \phi_k \rangle \quad (35)$$

$$\frac{\langle \phi_k, H_{\text{el}}^* \phi_k \rangle}{\langle \phi_k, \phi_k \rangle} = E_{\text{el},k} \geq E_0, \quad (36)$$

So, for any orthonormalized trial wave function $\tilde{\phi}$, with $\langle \phi_k, \phi_k \rangle = 1$, the task is to find \tilde{E}_{est} satisfying:

$$\tilde{E}_{\text{est}} = \min_{\tilde{\phi}} \{ \langle \phi_k, \phi_k \rangle \}. \quad (37)$$

To this end, define the orthonormal *Hartree-Fock basis* of single particle wave functions

$$\phi^{\text{HF}} := \{ \phi_i^{\text{HF}} \}_{i=1}^{N_e}.$$

Using this basis, (37) can be solved for any variation δ of ϕ in the following way:

$$\delta \left\{ \langle \tilde{\phi}, H_{\text{el}}^* \tilde{\phi} \rangle - \sum_{i=1}^{N_e} \epsilon_i^{\text{HF}} \left(\langle \tilde{\phi}_i, \tilde{\phi}_j \rangle - \delta_{ij} \right) \right\} \Big|_{\tilde{\phi}_j = \phi_j^{\text{HF}}} \stackrel{!}{=} 0 \quad \forall i, j \in \{1, \dots, N_e\}, \quad (38)$$

where ϵ_i^{HF} are Lagrangian multipliers to enforce orthonormality. Using functional derivatives, this can be written as

$$\frac{\delta}{\delta \tilde{\phi}_j} \left\{ \tilde{E}_{\text{el},j} - \sum_{i=1}^{N_e} \epsilon_i^{\text{HF}} \left(\int_{\mathbb{R}^3} [\tilde{\phi}_i t(\mathbf{x}_i) \tilde{\phi}_j(\mathbf{x}_j) d^3 \mathbf{x} - \delta_{ij}] \right) \right\} \Big|_{\tilde{\phi}_j = \phi_j^{\text{HF}}} = 0 \quad \forall j \in \{1, \dots, N_e\}.$$

After some calculations, we obtain

$$\left(-\frac{\hbar^2}{2m} \Delta_{\mathbf{x}} + V_{\text{e-n}} + V_{\text{H}} + V_{\text{X}} \right) \phi_i^{\text{HF}}(\mathbf{x}) = \epsilon_i^{\text{HF}} \phi_i^{\text{HF}}(\mathbf{x}), \quad \mathbf{x} \in \mathbb{R}^3, \quad (39)$$

in which the Hartree-Fock approximation of the density ρ is defined by

$$\rho^{\text{HF}}(\mathbf{x}) := \sum_{i=1}^{N_e} |\phi_i^{\text{HF}}(\mathbf{x})|^2, \quad \mathbf{x} \in \mathbb{R}^3,$$

with $\phi^{\text{HF}} = \phi_{\text{HF}}$. In (39), the *Hartree potential* is

$$V_{\text{H}}(\mathbf{x}) := \int_{\mathbb{R}^3} \frac{\rho^{\text{HF}}(\mathbf{x}')}{|\mathbf{x} - \mathbf{x}'|} d^3\mathbf{x}'$$

and the *exchange potential* is

$$V_{\text{X}}(\mathbf{x}) := \sum_{j=1}^{N_e} \int_{\mathbb{R}^3} \frac{\phi_i^{\text{HF}}(\mathbf{x}')\phi_j^{\text{HF}}(\mathbf{x}')}{|\mathbf{x} - \mathbf{x}'|} \phi_j^{\text{HF}}(\mathbf{x}) d^3\mathbf{x}'.$$

The equations (39) are called the *Hartree-Fock equations*, in which ϕ_i^{HF} are single-particle wave functions. Instead of having 1 equation involving N_e electrons, there are N_e equations involving one electron; these are still coupled via potentials. Although \tilde{E}_{est} are formally correct, the downside is that there is still deviation compared to experimental results. This deviation is due to the fact that the *correlation energy* is not taken into account. The correlation energy is a measure for how much the movement of a single electron is influenced by the other present electrons in a system. A third method, Density Functional Theory, will be discussed in the next section, which takes correlation into account.

4.3 Density Functional Theory

Instead of considering many-electron wave functions, a new approach has been presented to formulate the many-body problem in terms of the electron density ρ , since the latter, as opposed to the former, is a quantum observable. In this formulation, which is called *Density Functional Theory* (DFT), the electron density describes the system as a function of only three spatial coordinates as its variables, as opposed to the many-body wave function, which has $3N_e$ variables. In theory, DFT gives an exact solution for the density minimising the ground state energy. Until the 1990s, DFT has been deemed not accurate enough compared to experimental values; however, when the approximations for the exchange and correlation interactions had been improved, it became more popular among scientists. In Figure 9, the idea behind DFT is visualised.

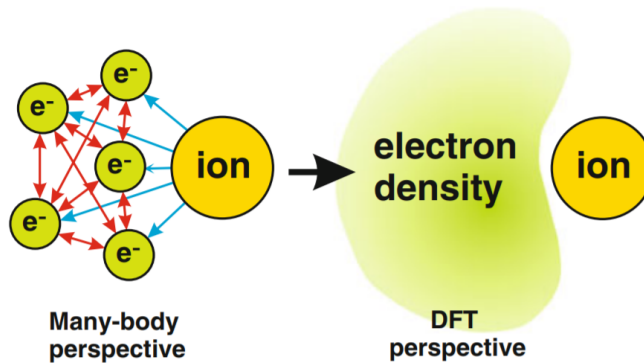


Figure 9: *The idea behind DFT: instead of taking the electrons as individually behaving particles their interactions are described via the electron density.* Source: [Friedhelm, J and Bechstedt, H2015]

4. ELECTRONIC STRUCTURE THEORY OF MANY-ELECTRON SYSTEMS

Instead of solving the electronic eigenvalue problem as in (35) and (36), the total energy of a system is described as a functional of the electron density ρ and one now solves:

$$E = \langle \phi_0, \hat{H}_{\text{el}}, \phi_0 \rangle$$

with $\hat{H}_{\text{el}} = T_e + V_{\text{e-e}} + V_{\text{ext}}$ and ϕ_0 is the Hartree-Fock ground state wave functions. Furthermore, $\rho(\mathbf{x})$ is the electron density defined by

$$\rho(\mathbf{x}) := \sum_{i=1}^{N_e} |\phi_i(\mathbf{x})|^2,$$

where $\hat{H}_{\text{el}} = T_e + V_{\text{e-e}} + V_{\text{ext}}$. Also, in practice we have that for the *external potential* $V_{\text{ext}} \rightarrow V_{\text{e-n}}$. The ground state ϕ_0 for \hat{H}_{el} depends on how V_{ext} is chosen. Because of the dependence on V_{ext} , there is a map defined by

$$\mathcal{C} : V_{\text{ext}} \mapsto \phi_0,$$

which is surjective, since the set of all possible ground-states ϕ_0 , are associated with V_{ext} . For the ground state wave functions, $\phi_0^i, i \in \mathbb{N}$ we get a second map:

$$\mathcal{D} : \phi_0 \mapsto \rho_{\phi_0},$$

which is again a surjective map. A schematic illustration of these *Hohenberg-Kohn maps* is shown in Figure 10.

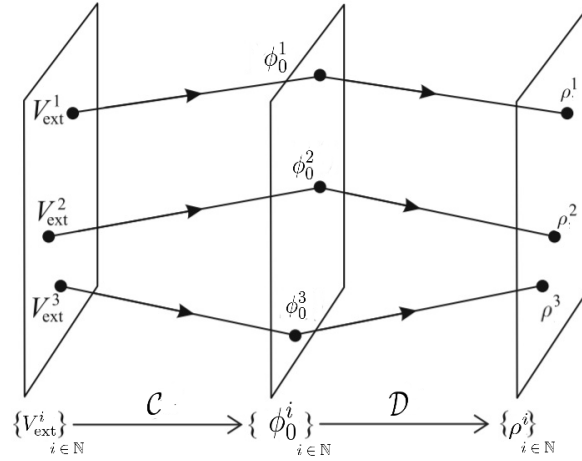


Figure 10: *Representation of the Hohenberg-Kohn maps \mathcal{C} and \mathcal{D} .* Source: [Friedhelm,J and Bechstedt, H2015]

The product of these maps $\mathcal{C} \cdot \mathcal{D}$ and the existence of its inverse $(\mathcal{C} \cdot \mathcal{D})^{-1}$ give us the *First Hohenberg-Kohn theorem*.

Theorem 7 (First Hohenberg-Kohn Theorem). *The total energy $E_0 = E_{\text{tot}}[\rho_0]$ in the ground state is a universal functional of the density ρ .*

In other words; there is a one-to-one correspondence between the *ground state density* ρ_0 of a system and the external potential V_{ext} acting on it. A proof of this can be found in [Friedhelm,J and Bechstedt, H2015], in which the assumption $V_{\text{ext}} \neq V_{\text{ext}} + \text{constant}$ are two different potential having the same ground state density is used to give a contradiction and thus two different potential cannot have the same ϕ_0 . For the *Second Hohenberg-Kohn theorem*, the variational character of the energy functional has to be proven.

Theorem 8 (Second Hohenberg-Kohn Theorem). *For a ground state ϕ_0 and a given external potential V_{ext} the energy functional $E_{\text{tot}}[\rho]$ assumes its global minimum value E_0 varying the density $\rho[\mathbf{x}]$ toward the true, minimal, ground state density $\rho_0(\mathbf{x})$, with E_0 defined by*

$$E_0 = \min_{\rho \rightarrow \rho_0} E_{\text{tot}}[\rho]. \quad (40)$$

Proof: Assume that the minimum occurs at a density $\rho_\phi \neq \rho_{\phi_0}$. Then, we have for the ground state energy,

$$E_0 = E_{\text{tot}}[\rho_0] \geq E_{\text{tot}}[\rho] = \langle \phi, \hat{H}_{\text{el}}, \phi \rangle.$$

However, because of the *Rayleigh-Ritz principle*, stating that $E_0 \leq E$ [Friedhelm,J and Bechstedt, H2015], we have

$$E_0 \leq E_{\text{tot}}[\rho].$$

Therefore, the assumption that the minimum occurs at a density $\rho \neq \rho_0$ is false, and indeed, the ground state energy can be determined by minimizing the energy functional as in was stated in (40). \square

The idea is again to find an observable, $\rho_0 = \rho_{\phi_0}$, such that

$$E[\rho] \xrightarrow{\rho \rightarrow \rho_0} E_0.$$

For the exact solution ρ_0 , we have that $E[\rho_0] = E_0$; However, in practice, it holds that $E[\rho] \geq E_0$. The energy $E[\rho]$ can be written as

$$E[\rho] = \langle \psi_0[\rho], \hat{H}_{\text{el}}, \psi_0[\rho] \rangle = \langle \psi_0[\rho], T_e[\rho], \psi_0[\rho] \rangle + \langle \psi_0[\rho], V_{\text{e-n}}[\rho], \psi_0[\rho] \rangle + \langle \psi_0[\rho], V_{\text{e-e}}[\rho], \psi_0[\rho] \rangle + \langle \psi_0[\rho], V_{\text{XC}}[\rho], \psi_0[\rho] \rangle,$$

in which $V_{\text{XC}}[\rho]$ is the *exchange-correlation potential*, with corresponding *exchange-correlation energy*, $E_{\text{XC}}[\rho]$. The *exchange energy* is the energy that is released in a system when two or more electrons exchange position, and the *correlation energy* is the difference between the exact energy and the Hartree-Fock energy.

Kohn and Sham⁵ constructed a refined approach of DFT, called *Kohn-Sham DFT*. In this approach, they use a better approximation for T_e . To this end we define the *Kohn-Sham wave functions* and *Kohn-Sham electron density* by

$$\phi^{\text{KS}} := \{\phi_i^{\text{KS}}\}_{i=1}^{N_e} \quad \rho_{\phi^{\text{KS}}}^{\text{KS}}(\mathbf{x}) = \sum_{i=1}^{N_e} |\phi_i^{\text{KS}}(\mathbf{x})|^2. \quad (41)$$

⁵Walter Kohn and Lu Jeu Sham developed Kohn-Sham DFT further from the two Hohenberg-Kohn Theorems. In 1998 they won the Nobel Prize in chemistry for it.

In theory the Kohn-Sham wave function ϕ^{KS} are chosen such that they produce the exact density, $\rho_{\phi^{\text{KS}}}^{\text{KS}} = \rho_{\phi}$. From now on, we will write $\rho_{\phi^{\text{KS}}}^{\text{KS}} = \rho^{\text{KS}}$. For Kohn-Sham DFT, $E_{\text{tot}}^{\text{KS}}$ can be written as

$$E_{\text{tot}}^{\text{KS}}[\rho^{\text{KS}}] := T_e^{\text{KS}}[\rho^{\text{KS}}] + E_{\text{e-n}}[\rho^{\text{KS}}] + E_{\text{e-e}}[\rho^{\text{KS}}] + \tilde{E}_{\text{XC}}[\rho^{\text{KS}}], \quad \text{with}$$

$$\tilde{E}_{\text{XC}}[\rho^{\text{KS}}] = E_{\text{XC}}[\rho^{\text{KS}}] + T_e[\rho^{\text{KS}}] - T_e^{\text{KS}}[\rho^{\text{KS}}],$$

where the approximation of the kinetic energy, $T_e^{\text{KS}}[\rho^{\text{KS}}]$, is defined by

$$T_e^{\text{KS}}[\rho^{\text{KS}}] := -\frac{1}{2m} \sum_{i=1}^{N_e} \int_{\mathbb{R}^3} \phi_i^{\text{KS}}(\mathbf{x}) \Delta \phi_i^{\text{KS}}(\mathbf{x}) d^3\mathbf{x}.$$

Furthermore, $E_{\text{e-e}}[\rho^{\text{KS}}]$ and $E_{\text{e-n}}[\rho^{\text{KS}}]$ are given by

$$E_{\text{e-e}}[\rho^{\text{KS}}] := \frac{1}{2} \int_{\mathbb{R}^3} \int_{\mathbb{R}^3} \frac{\rho^{\text{KS}}(\mathbf{x}) \rho^{\text{KS}}(\mathbf{x}')}{|\mathbf{x} - \mathbf{x}'|} d^3\mathbf{x} d^3\mathbf{x}',$$

$$E_{\text{e-n}}[\rho^{\text{KS}}] := \int_{\mathbb{R}^3} V_{\text{e-n}}[\rho^{\text{KS}}] \rho^{\text{KS}}(\mathbf{x}) d^3\mathbf{x}.$$

It must be mentioned that there are no exact values for $T_e[\rho^{\text{KS}}]$ and $E_{\text{XC}}[\rho^{\text{KS}}]$, only approximations. Since \tilde{E}_{XC} is approximated by E_{XC} , the difference is usually ignored.

Again we would like to minimize the energy $E_{\text{tot}}^{\text{KS}}$, which gives us

$$\frac{\delta E_{\text{tot}}^{\text{KS}}[\rho^{\text{KS}}]}{\delta \rho^{\text{KS}}} \stackrel{!}{=} 0.$$

Theorem 9. *The Kohn-Sham equations are given by*

$$\left[-\frac{\hbar^2}{2m} \Delta_{\mathbf{x}} + V_{\text{e-n}}[\rho^{\text{KS}}] + V_H[\rho^{\text{KS}}] + V_{\text{XC}}[\rho^{\text{KS}}] \right] \phi_i^{\text{KS}} = \epsilon_i^{\text{KS}} \phi_i^{\text{KS}}, \quad i \in \{1, \dots, N_e\}, \quad (42)$$

with

$$\frac{\delta E_{\text{XC}}}{\delta \rho^{\text{KS}}} = V_{\text{XC}}.$$

Proof: See [Arias2004], in which the first order of variation is used.

What one should keep in mind, is that equations (38) describe a fictional system of non-interacting particles. Also, the *Kohn-Sham energies* ϵ_i^{KS} are not physical energies, but Lagrange multipliers to enforce orthogonality. For now, we do have a way to compute $T_e^{\text{KS}}[\rho]$, but not to approximate $V_{\text{XC}}[\rho]$. Methods to do so are for instance Local Density Approximation (LDA) or Generalized Gradient Approximation (GGA), which will be discussed in the next section.

Advantage of DFT is that electron correlation is taken into account, and than it in theory has an exact solution. A disadvantage is that there are many functionals available for $V_{\text{XC}}[\rho]$, and it is not always clear what the best choice is for a certain system. For instance, one has to decide whether to focus more on a local approximation or on a global one. But even when this is decided, a wide range of functionals is available. [Standard2013]

4.4 Exchange-correlation energy approximations

Since $E_{\text{XC}}[\rho]$ and thus $V_{\text{XC}}[\rho]$ have no exact known form, they have to be approximated. The simplest approximation takes the exchange-correlation energy from a homogeneous electron gas: this is called the *Local Density Approximation* method. Its energy approximation reads

$$E_{\text{XC}}^{\text{LDA}}[\rho^{\text{KS}}](\mathbf{x}) := \int_{\mathbb{R}^3} \epsilon_{\text{XC}}[\rho^{\text{KS}}(\mathbf{x})] \rho^{\text{KS}}(\mathbf{x}) d^3\mathbf{x}. \quad (43)$$

It is common to split the *exchange-correlation energy density* ϵ_{XC} into two parts:

$$\epsilon_{\text{XC}}[\rho^{\text{KS}}] = \epsilon_{\text{X}}[\rho^{\text{KS}}] + \epsilon_{\text{C}}[\rho^{\text{KS}}],$$

where ϵ_{X} is the *exchange energy density* and ϵ_{C} the *correlation energy density*. The exchange energy density is given by the *Dirac functional*

$$\epsilon_{\text{X}}[\rho^{\text{KS}}] := -\frac{3}{4} \left(\frac{3}{\pi} \right)^{\frac{1}{3}} \rho^{\text{KS}}. \quad (44)$$

We now introduce the *Seitz radius* $r_{\text{s}}[\rho^{\text{KS}}]$, which is defined by:

$$r_{\text{s}}[\rho^{\text{KS}}(\mathbf{x})] = \left(\frac{3}{4\pi\rho^{\text{KS}}} \right)^{\frac{1}{3}}. \quad (45)$$

Using (45) in (44), we obtain: [Clark2003]

$$\epsilon_{\text{X}}[\rho^{\text{KS}}] = -\frac{3}{4} \left(\frac{9}{4\pi^2} \right)^{1/3} \frac{1}{r_{\text{s}}[\rho^{\text{KS}}]}. \quad (46)$$

For the correlation energy density ϵ_{C} , there are no corresponding expressions, but it can be determined accurately by Quantum Monte Carlo calculations and parametrizations. Quantum Monte Carlo calculations, are calculations based on the Quantum Monte Carlo experiments, which are computational algorithms relying on repeated random sampling to obtain numerical results. An example of a parametrization of the correlation energy is the following one by Ceperley. [Perdew1981] For $r_{\text{s}}[\rho^{\text{KS}}] \leq 0$, $\epsilon_{\text{C}}[r_{\text{s}}[\rho^{\text{KS}}]] \equiv 0$.

For $0 < r_{\text{s}}[\rho^{\text{KS}}] < 1$, we have

$$\epsilon_{\text{C}}[r_{\text{s}}[\rho^{\text{KS}}]] = \frac{\gamma}{1 + \beta_1 \sqrt{r_{\text{s}}[\rho^{\text{KS}}]} + \beta_2 r_{\text{s}}[\rho^{\text{KS}}]}, \quad (47)$$

with the quantum Monte Carlo parameters

$$\gamma = -0.1423, \quad \beta_1 = 1.0529, \quad \beta_2 = 0.3334.$$

For $r_{\text{s}}[\rho^{\text{KS}}] \geq 1$, $\epsilon_{\text{C}}[r_{\text{s}}[\rho^{\text{KS}}]]$ is given by

$$\epsilon_{\text{C}}[r_{\text{s}}[\rho^{\text{KS}}]] = A \log r_{\text{s}}[\rho^{\text{KS}}] + B + C r_{\text{s}}[\rho^{\text{KS}}] \log r_{\text{s}}[\rho^{\text{KS}}] + D r_{\text{s}}[\rho^{\text{KS}}], \quad (48)$$

with the quantum Monte Carlo parameters

$$A = 0.0311, \quad B = -0.048, \quad C = 0.0020, \quad D = -0.0016.$$

The exchange-correlation potential $V_{\text{XC}}^{\text{LDA}}$ [Perdew1981] is given by

$$V_{\text{XC}}^{\text{LDA}}[\rho] = \frac{\delta E_{\text{XC}}^{\text{LDA}}[\rho^{\text{KS}}]}{\delta[\rho^{\text{KS}}]} \approx \left(1 - \frac{r_s}{3} \frac{d}{dr_s}\right) \epsilon_{\text{XC}}[r_s]. \quad (49)$$

In order to improve the LDA, it is sometimes assumed that E_{XC} does not only depend on the density, ρ , but also on its gradients $\nabla_{\mathbf{x}}\rho$. This method is known as the *Generalized Gradient Approximation* (GGA). When taking also $\nabla_{\mathbf{x}}^2, \dots, \nabla_{\mathbf{x}}^n$ $n \in \mathbb{N}_{n \geq 2}$ into account, one arrives at the family of functionals known as the *GGAs*. Here, $E_{\text{XC}}^{\text{GGA}}$ can be written as a functional of

$$E_{\text{XC}}^{\text{GGA}} = E_{\text{XC}}^{\text{GGA}}[\rho(\mathbf{x}), \nabla_{\mathbf{x}}\rho(\mathbf{x}), \dots, \nabla_{\mathbf{x}}^n\rho(\mathbf{x})]. \quad \text{for some } n \in \mathbb{N}.$$

4.5 Summary

For general molecular systems, solutions to the Schrödinger equation have to be approximated numerically. There are several methods, which each have advantages and disadvantages. Among these methods, DFT is the most popular because it is quite accurate and not computationally expensive. Also, DFT formally has in theory an exact solution. Besides this, it takes electron correlation into account, which the Born-Oppenheimer approximation and the Hartree-Fock method did not. The downside of DFT is that there are many approximations possible for V_{XC} and it is not always clear which one to choose. An example of such an approximation is LDA, which has several improvements itself, known as the GGAs. In the next chapter, DFT will be applied on single atoms.

5 Application of DFT to single atoms

In the previous chapter, DFT has been discussed. Now, we will look at an example of DFT applied on single atoms. For hydrogen, it is possible to obtain the wave function analytically; however, for large atoms this is no longer possible. Therefore, an approximation is needed, which is chosen to be DFT in this chapter. For approximating the wave functions, the *Numerov's method* will be used. The Numerov method⁶ is a method to solve ordinary differential equations of the form

$$\frac{d^2 y}{dx^2}(x) = g(x)y(x) + s(x), \quad x \in \mathbb{R}. \quad (50)$$

We would like to write the Schrödinger equation in this form as well. Because of the angular symmetries in Lemma 15, only for the radial part a numerical approximation is needed. To this end, we choose the following form for the radial wave function R_{nl} :

$$R_{nl}(r) = \frac{1}{r} U_{nl}(r) \quad \text{for some function } U_{nl}(r). \quad (51)$$

The *radial electron density* is defined as [Schr2011]

$$\rho^*(r) := \frac{1}{4\pi} \sum_{n=1}^{N_e} \sum_{l=-n}^n \left| \frac{U_{nl}(r)}{r} \right|^2. \quad (52)$$

When substituting (51) in (9), we obtain the following relation:

$$\begin{aligned} \Delta_r R_{nl}(r) &= \Delta_r \left(\frac{1}{r} U_{nl}(r) \right) = \frac{1}{r^2} \frac{d}{dr} \left(r^2 \frac{d}{dr} \left(\frac{1}{r} U_{nl}(r) \right) \right) \\ &= \frac{1}{r^2} \frac{d}{dr} \left(-U_{nl}(r) + r \frac{d}{dr} U_{nl}(r) \right) \\ &= \frac{1}{r^2} \left(-\frac{d}{dr} U_{nl}(r) + \frac{d}{dr} U_{n,l}(r) + r \frac{d^2}{dr^2} U_{nl}(r) \right) \\ &= \frac{1}{r} \frac{d^2}{dr^2} U_{nl}(r). \end{aligned}$$

This gives for (9), with a general potential $V = V(r)$:

$$-\frac{\hbar^2}{2m} \frac{d^2}{dr^2} U_{nl}(r) + \left(\frac{\hbar^2}{2m} \frac{l(l+1)}{r^2} + V(r) \right) U_{nl}(r) = E_n U_{nl}(r).$$

By rewriting this, we have

$$\frac{d^2}{dr^2} U_{nl}(r) = g(r) U_{nl}(r), \quad (53)$$

where

$$g(r) = \frac{l(l+1)}{r^2} + \frac{2m}{\hbar^2} V(r) - E_n. \quad (54)$$

⁶This method has been developed by Boris Vasil'evich Numerov, who was a Russian astronomer.

5. APPLICATION OF DFT TO SINGLE ATOMS

When using a Taylor series expansion to approximate $\frac{d^2}{dr^2}U_{nl}(r)$ for a linear grid of the form $r_k = r_0 + kh$, with $k \in \mathbb{N}_0$, stepsize h and $r_0 = 0$, this results in the following:

$$U_{nl}^{k+1} + U_{nl}^{k-1} - 2U_{nl}^k = h^2 \frac{d^2 U_{nl}(r_k)}{dr^2} + \frac{h^4}{12} \left(\frac{d^2 U_{nl}(r_{k+1})}{dr^2} + \frac{d^2 U_{nl}(r_{k-1})}{dr^2} - 2 \frac{d^2 U_{nl}(r_k)}{dr^2} \right) + \mathcal{O}(h^6), \quad (55)$$

where $U_{nl}^i := U_{nl}(r_i)$. If we define $g^i := g(r_i)$, use (53) and a similar expansion for the second derivative of $U(r)$, we get

$$\left(1 - \frac{h^2}{12}g^{i+1}\right)U_{nl}^{i+1} + \left(1 - \frac{h^2}{12}g^{i-1}\right)U_{nl}^{i-1} - \left(2 + \frac{5h^2}{6}g^i\right)U_{nl}^i = \mathcal{O}(h^6). \quad (56)$$

This is called the *Numerov relation*. Sometimes, it is more convenient to use a logarithmic grid: for example, when looking at an atom or molecule. For molecular systems, we want many grid points close to the nucleus (the origin), and a decreasing amount further away from it, in accordance with the rapid decay of the wave function. The logarithmic grid has the form

$$r_n = r_0 e^{nh}. \quad (57)$$

When applying the coordinate transformation $r = r_0 e^u$ with $u := nh$ on $U_{nl}(u)$, it can be derived that [Schr2011]

$$\frac{d^2 U_{nl}(u)}{du^2} = (\log(r_0))^2 (l(l+1) + 2(V(u) - E_n)u^2) U_{nl}(u). \quad (58)$$

Solving (58) can be done with a numerical scheme and using *forward and backward iteration*. An example of such a scheme is *Adam's extrapolation and interpolation*. [Abramowitz et al.1972] For *Adams extrapolations*; we have forward and backward extrapolation respectively

$$U_{nl}^{k+1} = U_{nl}^k + \frac{h}{24} \left(55U_{nl}^{k'} - 59U_{nl}^{k-1'} + U_{nl}^{k-2'} - 9U_{nl}^{k-3'} \right), \quad (59)$$

and

$$U_{nl}^{k-1} = U_{nl}^k - \frac{h}{24} \left(55U_{nl}^{k'} - 59U_{nl}^{k+1'} + 37U_{nl}^{k+2'} - 9U_{nl}^{k+3'} \right), \quad (60)$$

in which $U_{nl}^{i'k} = U_{nl}(u_k)$ For *Adams interpolation*, the forward and backward interpolation scheme is given by

$$U_{nl}^{k+1} = U_{nl}^k + \frac{h}{24} \left(9U_{nl}^{k+1'} + 19U_{nl}^{k'} - 5U_{nl}^{k-1'} + U_{nl}^{k-2'} \right), \quad (61)$$

and

$$U_{nl}^{k+1} = U_{nl}^k - \frac{h}{24} \left(9U_{nl}^{k-1'} + 19U_{nl}^{k'} - 5U_{nl}^{k+1'} + U_{nl}^{k+2'} \right). \quad (62)$$

When using (59) - (62) twice, the radial wave functions can be approximated.

For this formulation, a model is made and applied on a carbon atom. A carbon atom has six electrons: two core electrons and four valence electrons, and the electron configuration is given by $1s^2 2s^2 2p^2$. In this model, the LDA approximation described in §4.4 is used for the exchange-correlation potential, and (59) - (62) are used to find the radial wave functions.

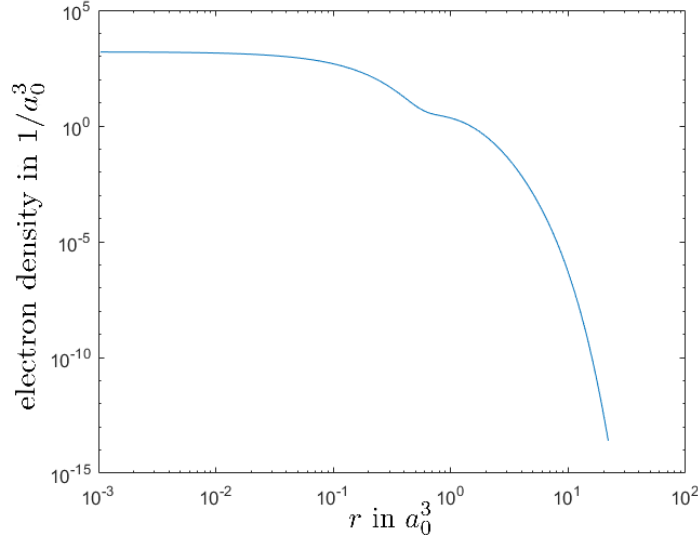


Figure 11: *Radial electron density for the carbon atom on a logarithmic scale.*

In this plot, the distance is in *Hartree units*, $e^2 = \hbar = m = 1$, with $a_0 = 5.29 \cdot 10^{-11}$ m, which is also called the *Bohr radius*. [Pask2013] When looking at Figure 11, it can be seen that the electron density decays further away from the origin, $r = 0$ where the nucleus is placed. Around $r = 1a_0$, there is a sudden drop, which is due to the fact that the radial wave functions cancel each other a bit out at this point. The individual radial wave functions R_{10} , R_{20} and R_{21} , for each orbital of the carbon atom are plotted in Figure 12.

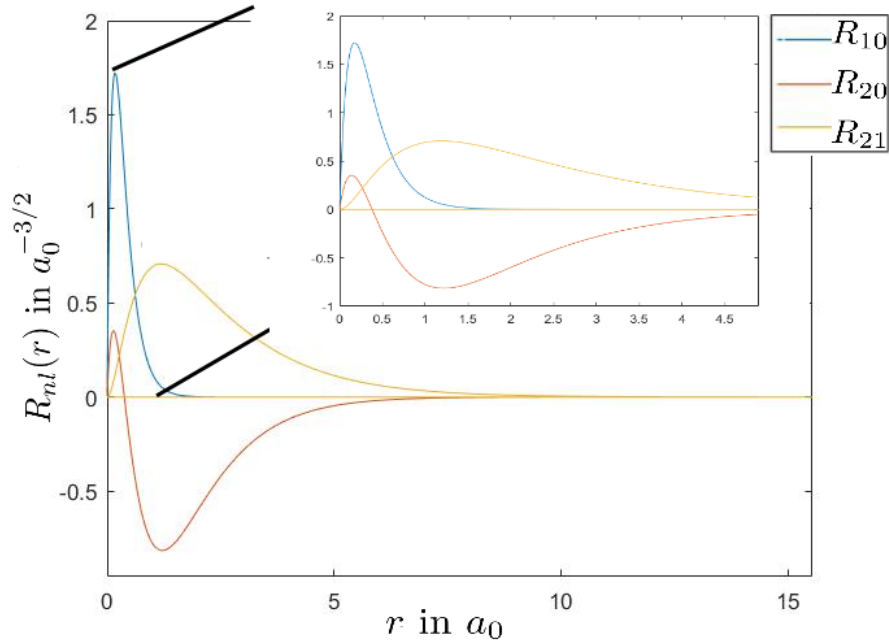


Figure 12: *Radial wave functions R_{10} , R_{20} and R_{21} for the carbon atom.*

5. APPLICATION OF DFT TO SINGLE ATOMS

The number of radial roots for a radial wave function is $n - 1 - l$. [Urone2019] At these roots, the radial wave function is zero and the function changes sign. To clarify this, for R_{10} , $1s^2$, and R_{20} , $2s^2$, the difference in shape is shown in Figure 13.

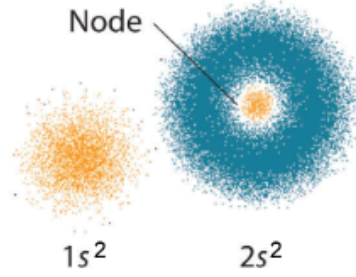


Figure 13: *Nodes for wave functions corresponding to $1s^2$ and $2s^2$ orbitals. Source: [Urone2019]*

The ground-state energies of each of the radial wave functions are depicted in Table 1. The computed energies are in Hartree units (Ha), which can be converted to electronvolts via $1 \text{ Ha} = 27.2116... \text{ eV}$.

Wave function	Energy (Ha)	Energy (eV)
$R_{10}(r)$	-9.9505	-270.6528
$R_{20}(r)$	-0.5013	-13.6364
$R_{21}(r)$	-0.1992	-5.4191

Table 1: *The radial wave functions with corresponding ground-state energies (referred to as Energy).*

Here, the further away the electron is from the nucleus, the less influence the nucleus has on the electron and less energy is needed to remove an electron from its orbital. As n and l increase, the further away it is from the nucleus and the higher the ground state energy.

6 Coarse-Graining Density Functional Theory

In the previous chapter, an overview of Density Functional Theory has been given. However, this method solves for individual orbitals: so, when having individual particle wave functions for a very large number of atoms, this method is computationally expensive. Because of this, approximation methods with less computation costs have been sought of, for DFT the computation costs are $\mathcal{O}(N_e^3)$. In this chapter, *Coarse-Grained Density Functional Theory* (CGDFT), is discussed and reformulated for single atoms, based on [Suryanarayana et al.2013]. This approximation method consists of two steps. The first step consists of a linear-scaling method, called the *Linear-Scaling Spectral Gauss Quadrature* (LSSGQ) *Method*, via which the electron density can be evaluated: just like for DFT, it is not needed to take individual orbitals into account. The second step, the coarse-graining step, introduces a spatial approximation scheme which is designed to have a high resolution near the nuclei and vice versa. Although the method being developed to have a high resolution for large molecular systems, we reformulate it later specifically for single atoms, in order to analyse the method on atomic scale.

We start this by making a guess for the positions of the nuclei, and then obtain the electron density and compute the ground state energy. To further minimize the energy with respect to the position of the nuclei, we have

$$f_J = - \int_{\mathbb{R}^3} \frac{\partial b_J(\mathbf{x}, \mathbf{R}_J)}{\partial \mathbf{R}_J} (\phi(\mathbf{x}, \mathbf{R}) - \phi_J(\mathbf{x}, \mathbf{R}_J)), \quad (63)$$

with $\phi_J(\mathbf{x}, \mathbf{R}_J) = \int_{\mathbb{R}^3} \frac{b_J(\mathbf{x}', \mathbf{R}_J)}{|\mathbf{x} - \mathbf{x}'|} d\mathbf{x}'$ and f_J is the force on the J^{th} nucleus. For a given position \mathbf{R} of the nuclei, the ground-state energy is obtained as a solution of the variational principle

$$\mathcal{E}_0(\mathbf{R}) = \inf_{\psi} \mathcal{E}(\psi, \mathbf{R}).$$

Now we will focus on the electrons and come back to this later.

Without loss of generality, it is assumed that N_e is even. Furthermore, Z is the number of protons in a core. We also use Hartree units, $e^2 = \hbar = m = 1$, to this end. The electrostatic-potential terms V_{ext} and $V_{\text{e-e}}$, can be rewritten to one term κ , which solves a Poisson equation:

$$-\frac{1}{4\pi} \Delta_{\mathbf{x}} \kappa(\mathbf{x}, \mathbf{R}) = \tilde{\rho}(\mathbf{x}) + b(\mathbf{x}, \mathbf{R}), \quad \tilde{\rho}(\mathbf{x}) := 2 \sum_{n=1}^{N_e/2} |\psi_n(\mathbf{x})|^2 \quad (64)$$

in which $b(\mathbf{x}, \mathbf{R})$ denotes the *charge density of the nuclei* and $\tilde{\rho} = \rho^{KS}$ the Kohn-Sham electron density, an approximation for it will later be proposed. A proof of this is given in [Ismail-Beigi2000]. Solving (64) numerically, using a three-dimensional finite difference method on a uniform grid with step size h such that $x_n = x_0 + nh$, $y_n = y_0 + nh$ and $z_n = z_0 + nh$, we obtain for all $n \in \mathbb{Z}$

$$\forall n : -\frac{1}{4\pi} \frac{1}{h^2} \left(\kappa^{n+1,n,n} + \kappa^{n-1,n,n} + \kappa^{n,n+1,n} + \kappa^{n,n-1,n} + \right. \\ \left. \kappa^{n,n,n+1} + \kappa^{n,n,n-1} - 6\kappa^{n,n,n} \right) = \rho^{n,n,n} + b^{n,n,n}, \quad (65)$$

with $f^{i,j,k} = f(x_i, y_j, z_k)$, where $f \in \{\kappa, \rho, b\}$.

In molecular systems, the *core electrons*, the electrons closest to the core, are *chemically inactive*, meaning they do not move or react; therefore, they have little contribution towards determining physical properties. In order to have a simplified approximation of a molecular system, a *pseudo-potential* $V_{\text{ext}}^{\text{PS}}(\mathbf{x}, \mathbf{R})$ can be used to describe the effect of these core electrons. Note that $V_{\text{ext}}^{\text{PS}}(\mathbf{x}, \mathbf{R})$ approaches $V_{\text{e-n}}(\mathbf{x}, \mathbf{R})$.

In the formulation of CGDFT, we have the following Ansatz.

Ansatz 3.

$$b(\mathbf{x}, \mathbf{R}) = -\frac{1}{4\pi} \Delta_{\mathbf{x}} V_{\text{ext}}^{\text{PS}}(\mathbf{x}, \mathbf{R}). \quad (66)$$

Because of this Ansatz, we have an approximation for κ , we introduce $\tilde{\kappa}$.

6.1 The key idea of the reformulation of DFT

For the reformulation of DFT, we have the following eigenvalue problem:

$$H\psi_n(\mathbf{x}) = \lambda_n(\mathbf{R})\psi_n(\mathbf{x}), \quad (67)$$

The Hamiltonian H from (67) reads (in Hartree units)

$$H := -\frac{1}{2} \Delta_{\mathbf{x}} + V_{\text{XC}}[\tilde{\rho}](\mathbf{x}) + \tilde{\kappa}(\mathbf{x}, \mathbf{R}).$$

Now, H is a self-adjoint operator, because of Theorem 5, and has eigenvalues λ_n , $n \in \{1, \dots, N_e\}$ from which we pick the first $N_{e/2}$, which are ordered: $\lambda_1 \leq \lambda_2 \leq \dots \lambda_{N_{e/2}}$. For $V_{\text{XC}}[\rho]$ we choose the LDA as described in §4.4.

The key idea of the reformulation of DFT is that the ground-state energy, E_0 , does not depend on individual eigenvalues and eigenvectors, but on sums. The sums for the *band structure energy* U_{band} and electron density $\tilde{\rho}$ are respectively given by:

$$\tilde{U}_{\text{band}}(\mathbf{R}) := 2 \sum_{n=1}^{N_{e/2}} \lambda_n(\mathbf{R}), \quad \tilde{\rho}(\mathbf{x}) := 2 \sum_{n=1}^{N_{e/2}} |\psi_n(\mathbf{x})|^2. \quad (68)$$

These sums will later be sampled and weighted, as approximation for the band structure energy and electron density. Since the wave functions are normalized, we have for the electron density:

$$N_e = \int_{\mathbb{R}^3} \tilde{\rho}(\mathbf{x}) d^3 \mathbf{x}. \quad (69)$$

Furthermore, we have $b(\mathbf{x}, \mathbf{R}) = \sum_{J=1}^{N_\alpha} b_J(\mathbf{x}, \mathbf{R}_J)$. Because $V_{\text{XC}}[\tilde{\rho}]$ also depend on $\tilde{\rho}$, the ground-state energy $E_0[\tilde{\rho}]$ also depends on $\tilde{\rho}$, and is calculated by evaluating [Suryanarayana et al.2013]

$$\begin{aligned} \mathcal{E}_0[\tilde{\rho}](\mathbf{R}) = & U_{\text{band}} + E_{\text{XC}}[\tilde{\rho}] + \frac{1}{2} \int_{\mathbb{R}^3} (b(\mathbf{x}, \mathbf{R}) - \tilde{\rho}(\mathbf{x})) \kappa(\mathbf{x}, \mathbf{R}) d^3 \mathbf{x} - \\ & \int_{\mathbb{R}^3} V_{\text{XC}}[\tilde{\rho}](\mathbf{x}) \tilde{\rho}(\mathbf{x}) d^3 \mathbf{x} - \frac{1}{2} \sum_{J=1}^{N_\alpha} \int_{\mathbb{R}^3} \int_{\mathbb{R}^3} \frac{b(\mathbf{x}, \mathbf{R}_J) b(\mathbf{x}', \mathbf{R}_J)}{|\mathbf{x} - \mathbf{x}'|} d^3 \mathbf{x} d^3 \mathbf{x}'. \end{aligned} \quad (70)$$

Next, we introduce the *orbital occupation function*, defined by

$$g(\lambda; \lambda_f) := \mathbb{1}_{\{\lambda \leq \lambda_f\}}, \quad (71)$$

where $\lambda_f := \lambda_{N_e/2}$ is the *Fermi energy*, which can be calculated using the relation

$$N_e \stackrel{!}{=} 2 \sum_{n=1}^{N_e/2} g(\lambda_n; \lambda_f). \quad (72)$$

Now, U_{band} and $\tilde{\rho}(\mathbf{x})$ can be rewritten to, see [Suryanarayana et al.2013]

$$U_{\text{band}} = 2 \sum_{n=1}^{N_e/2} \lambda_n g(\lambda_n; \lambda_f), \quad \tilde{\rho}(\mathbf{x}) = 2 \sum_{n=1}^{N_e/2} g(\lambda_n; \lambda_f) |\psi_n(\mathbf{x})|^2. \quad (73)$$

The orbital occupation function can also be extended to finite temperatures:

$$g_\sigma(\lambda; \lambda_f) := \frac{1}{1 + \exp\left(\frac{\lambda - \lambda_f}{\sigma}\right)}, \quad (74)$$

where $\sigma = k_B \theta$ in Joules, $k_B = 1.380649 \cdot 10^{-23} \text{J K}^{-1}$ the Boltzmann constant and θ the *absolute temperature* in Kelvin. For the finite temperature extension, (72) still holds due to spectral theory. In this finite temperature extension, the *ground-state Helmholtz free-energy* is given by

$$\mathcal{F}[\tilde{\rho}](\mathbf{R}) := \mathcal{E}_0^\sigma[\tilde{\rho}](\mathbf{R}) - \theta \mathcal{S}^\sigma, \quad (75)$$

where $\mathcal{E}_0^\sigma[\tilde{\rho}](\mathbf{R})$ is the finite temperature counterpart of the ground-state energy at absolute zero \mathcal{E}_0 , and is defined by (70) with $g_\sigma(\lambda; \lambda_f)$ instead of $g(\lambda; \lambda_f)$.

The *entropy* \mathcal{S}^σ , which is the amount of disorder in a system, is given by

$$\mathcal{S}^\sigma := -2k_B \sum_{n=1}^{N_e/2} [g_\sigma(\lambda_n; \lambda_f) \log(g_\sigma(\lambda_n; \lambda_f)) + (1 - g_\sigma(\lambda_n; \lambda_f)) \log(1 - g_\sigma(\lambda_n; \lambda_f))], \quad (76)$$

in which \mathcal{S} results from the fractional orbital occupations due to the formulation of g_σ in (74).

In CGDFT, one considers rather the collective result of the orbitals than the individual ones. So, we now sample and weight the sums in (68) for values $1, \dots, K$: with $K \ll N_e/2$. This results in

$$\hat{U}_{\text{band}}(\mathbf{R}) := 2 \sum_{k=1}^K \hat{w}_k \hat{\lambda}_k(\mathbf{R}) g_\sigma(\hat{\lambda}_k; \lambda_f), \quad \hat{\rho}(\mathbf{x}) := 2 \sum_{k=1}^K \hat{w}_k g_\sigma(\hat{\lambda}_k; \lambda_f), \quad (77)$$

where $\hat{\lambda}_k$ and \hat{w}_k are *Gaussian Quadrature* points, which will be discussed in the following section.

6.2 Linear-Scaling Spectral Gaussian Quadrature Method

In this section, the *Linear-Scaling Spectral Gaussian Quadrature (LSSGQ) Method* is discussed and used to find values for the quadrature nodes $\hat{\lambda}_k$ and weights \hat{w}_k . The eigenvalue problem is given by:

$$H[\hat{\rho}](\mathbf{R})\psi_n(\mathbf{x}) = \left(-\frac{1}{2}\Delta_{\mathbf{x}} + V_{\text{all}}[\hat{\rho}](\mathbf{x}, \mathbf{R}) \right) \psi_n(\mathbf{x}) = E_n(\mathbf{R})\psi_n(\mathbf{x}) \quad (78)$$

with

$$V_{\text{all}}[\hat{\rho}](\mathbf{x}, \mathbf{R}) := V_{\text{XC}}[\hat{\rho}](\mathbf{x}) + \kappa(\mathbf{x}, \mathbf{R}).$$

The wave function $\psi_n(\mathbf{x}, \mathbf{R})$ does not depend on \mathbf{R} , since the wave function gives us only information about the electrons. By discretizing the Laplacian, the eigenvalue problem is given by

$$\mathbf{H}(\mathbf{R})\psi_n = \lambda_n(\mathbf{R})\psi_n, \quad n = 1, 2, \dots, N_{e/2} \quad (79)$$

in which \mathbf{H} is the discretized variant of H in (78), N_d is the grid size $\psi_n = [\psi_n^1, \psi_n^2, \dots, \psi_n^{N_d^3}]$ is the n^{th} eigenfunction or orbital, ψ_n^p is the value of the n^{th} orbital at node \mathbf{x}^p with $p \in \{1, \dots, N_d^3\}$. The grid is 3D and has a size of N_d in all three directions, so *grid size* \times *grid size* \times *grid size*. When using the three-dimensional central difference approximation, we have for $m \in \{2, \dots, N_d - 1\}$

$$\Delta_{\mathbf{x}}\psi_n(\mathbf{x}) \doteq \frac{1}{h^2} \left(\psi_n^{m+1,m,m} + \psi_n^{m-1,m,m} + \psi_n^{m,m+1,m} + \psi_n^{m,m-1,m} + \psi_n^{m,m,m+1} + \psi_n^{m,m,m-1} - 6\psi_n^{m,m,m} \right). \quad (80)$$

The nodes are ordered such that $\psi_n^{1,1,1} = \mathbf{x}^1, \psi_n^{2,1,1} = \mathbf{x}^2, \dots, \psi_n^{N_d, N_d, N_d-1} = \mathbf{x}^{N_d^3-1}, \psi_n^{N_d, N_d, N_d} = \mathbf{x}^{N_d^3}$. Using this, the following matrix equation corresponds to the eigenvalue problem:

$$\begin{aligned}
 & -\frac{1}{2h^2} \begin{pmatrix} -6 & 1 & & 1 & & 1 & & \\ 1 & -6 & 1 & & 1 & & \ddots & \\ & \ddots & \ddots & \ddots & & \ddots & & 1 \\ 1 & & 1 & -6 & 1 & & \ddots & \\ & \ddots & & \ddots & \ddots & \ddots & & 1 \\ 1 & & \ddots & & 1 & -6 & 1 & \\ & \ddots & & \ddots & & 1 & -6 & 1 \\ & & 1 & & 1 & & 1 & -6 \end{pmatrix} \begin{pmatrix} \psi_n^1 \\ \psi_n^2 \\ \vdots \\ \vdots \\ \vdots \\ \vdots \\ \psi_n^{N_d^3} \end{pmatrix} \\
 & + \begin{pmatrix} V_{\text{all},1}[\hat{\rho}](\mathbf{x}^1) & & & & & & \\ & V_{\text{all},2}[\hat{\rho}](\mathbf{x}^2) & & & & & \\ & & \ddots & & & & \\ & & & V_{\text{all},N_d^3-1}[\hat{\rho}](\mathbf{x}^{N_d^3-1}) & & & \\ & & & & V_{\text{all},N_d^3}[\hat{\rho}](\mathbf{x}^{N_d^3}) & & \end{pmatrix} \begin{pmatrix} \psi_n^1 \\ \psi_n^2 \\ \vdots \\ \vdots \\ \psi_n^{N_d^3} \end{pmatrix} \\
 & = E_n(\mathbf{R}) \begin{pmatrix} \psi_n^1 \\ \psi_n^2 \\ \vdots \\ \vdots \\ \psi_n^{N_d^3} \end{pmatrix}, \tag{81}
 \end{aligned}$$

in which $V_{\text{all},p}[\hat{\rho}](\mathbf{x}^p)$ is the potential in node p . The distance from the diagonal to the second subdiagonal of ones is N_d and the distance to the third subdiagonal of ones is N_d^2 . It should be mentioned that in $V_{\text{all}}[\hat{\rho}](\mathbf{x})$, for $V_{\text{XC}}[\hat{\rho}](\mathbf{x})$ the LDA described in §4.4 is used.

When using a *Lanczos-type iteration* to obtain the Gaussian quadrature nodes $\hat{\lambda}_k$ and weights \hat{w}_k , which is described below and more detailed for general eigenvalue problems in [Suryanarayana et al.2013], the following is done:

$$\forall k, p \quad b_{k+1}^p \mathbf{v}_{k+1}^p = (\mathbf{H} - a_{k+1}^p) \mathbf{v}_k^p - b_k^p \mathbf{v}_{k-1}^p, \quad k \in \{0, 1, \dots, K-1\}, \tag{82}$$

$$\mathbf{v}_{-1}^p = \mathbf{0}, \quad \mathbf{v}_0^p = \mathbf{e}_p, \quad \text{with } \mathbf{v}_k^p \in \mathbb{R}^{N_d^3}, \quad \text{and } b_0^p = 1, \tag{83}$$

where \mathbf{e}_p is the unit vector, with $\mathbf{e}_p^i := \delta_p^i \quad \forall i \in \{1, \dots, N_d^3\}$. In this iteration, a_{k+1}^p is computed as follows:

$$a_{k+1}^p = \mathbf{v}_k^{p\top} \mathbf{H} \mathbf{v}_k^p, \quad k \in \{0, 1, \dots, K-1\}$$

and b_k^p such that

$$\|\mathbf{v}_k^p\|_2^2 = \sum_{i=1}^{N_d} \mathbf{v}_{ki}^{p^2} = 1.$$

Next, the values a_{k+1}^p and b_{k+1}^p are stored in the following *tridiagonal Jacobian* matrix to

obtain the Gaussian quadrature nodes and weights:

$$\hat{J}_K^p = \begin{pmatrix} a_1^p & b_1^p & & & \\ b_1^p & a_2^p & b_2^p & & \\ & \ddots & \ddots & \ddots & \\ & & b_{K-2}^p & a_{K-1}^p & b_{K-1}^p \\ & & & b_{K-1}^p & a_K^p \end{pmatrix} \quad (84)$$

Now, it is possible to use the Gaussian quadrature rule and to calculate the *spectral Gaussian quadrature nodes* $\{\hat{\lambda}_k^p\}_{k=1}^K$ and *weights* $\{\hat{w}_k^p\}_{k=1}^K$. It is called *spectral* quadrature nodes, because of the spectral theory that is behind it; a more detailed background on spectral theory can be found in [Suryanarayana et al.2013] and [Rudin1991]. The eigenvalues of \hat{J}_k^p are the nodes $\{\hat{\lambda}_k^p\}_{k=1}^K$ and the squares of the first elements of the normalized eigenvectors are the weights $\{\hat{w}_k^p\}_{k=1}^K$ of the Gaussian quadrature rule. It is important to mention that for each node $p \in \{1, \dots, N_d^3\}$, the Gaussian quadratures of the nodes and weights can be computed individually.

Because the nodes $\{\hat{\lambda}_k^p\}_{k=1}^K$ and weights $\{\hat{w}_k^p\}_{k=1}^K$ are known now, the Fermi energy can be approximated by solving for the constraint

$$N_e \stackrel{!}{=} 2 \sum_{p=1}^{N_d^3} \sum_{k=1}^K \hat{w}_k^p g_\sigma(\hat{\lambda}_k^p; \lambda_f). \quad (85)$$

This can be derived from condition (72), together with the use of spectral theory, which can be found in [Suryanarayana et al.2013].

Similary, the band structure energy from (73) and the entropy from (76) can be approximated as well:

$$\hat{U}_{\text{band}}^\sigma(\mathbf{R}) \approx 2 \sum_{p=1}^{N_d^3} \sum_{k=1}^K \hat{w}_k^p \hat{\lambda}_k^p(\mathbf{R}) g_\sigma(\hat{\lambda}_k^p; \lambda_f), \quad (86)$$

$$\mathcal{S} \approx -2k_B \sum_{p=1}^{N_d^3} \sum_{k=1}^K \hat{w}_k^p [g_\sigma(\hat{\lambda}_k^p; \lambda_f) \log(g_\sigma(\hat{\lambda}_k^p; \lambda_f)) + (1 - g_\sigma(\hat{\lambda}_k^p; \lambda_f)) \log(1 - g_\sigma(\hat{\lambda}_k^p; \lambda_f))]. \quad (87)$$

Note that (85), (86) and (87) also hold for g and g_σ is replaced by g . When the Fermi energy is obtained, the electron density $\hat{\rho}(\mathbf{x}^p)$ for each p can be calculated. When comparing this density to the one starting in (64), a new electron density, starting over from (64) can be calculated until convergence of the electron density is reached. Note that during this update, one has to make sure that the electron density is normalized as in (69). When the electron density has converged, the ground-state energy can be computed. After this a new guess for the position of the nuclei is generated until the energy is minimized with respect to the position of the atoms. Lastly, the Helmholtz free energy can be computed by using (75) and (87). When writing the steps out in an algorithm, we get the following scheme:

Generate guess for positions of the nuclei (\mathbf{R})

repeat

 Calculate charge density of the nucleus $b(\mathbf{x}, \mathbf{R})$, (66);

 Generate a guess for electron density $\rho(\mathbf{x})$ (later, an example will be given);

for each \mathbf{x}^p , $p \in \{1, \dots, N_d^3\}$ **do**

repeat

 Calculate the electrostatic potential $\tilde{\kappa}(\mathbf{x}, \mathbf{R})$, (64);

 Calculate the exchange correlation potential $V_{\text{XC}}[\hat{\rho}]$, §4.4;

 Discretize the Hamiltonian, (81);

 Calculate the Gaussian quadrature nodes and weights, (84);

 Calculate the Fermi energy, (85);

 Normalize and update the electron density $\hat{\rho}$;

until convergence of electron density;

end

 Evaluate ground-state energy, using (70) and (86);

 Calculate forces on the nuclei, using (63);

until Energy minimized with respect to position of atoms;

Evaluate the entropy and Helmholtz free energy, using (75) and (87).

Algorithm 1: LSSGQ method.

6.3 Formulation of CGDFT

We denote the set of all nodes $\{\mathbf{x}^p\}, p \in \mathcal{N} = \{1, \dots, N_d^3\}$. Recall that $\{\hat{\lambda}_k^p\}_{k=1}^K$ and $\{\hat{w}_k^p\}_{k=1}^K$ can be computed individually for each of these nodes p , which is the key idea behind CGDFT. Since the density is high around the vicinity of the origin and decays away from it, we want many evaluation points \mathbf{x}^p in the vicinity of the origin. This is why a set of *representative nodes* $\{\mathbf{x}^q\} \mathcal{R} \subseteq \mathcal{N}$ is chosen to be evaluated according to the LSSGQ method; for the non-representative nodes, the following decompositions are used to evaluate the electron density, the band structure energy and the entropy:

$$\hat{\rho}|_{\mathcal{N} \setminus \mathcal{R}} = \hat{\rho}^0 + \hat{\rho}^d, \quad \hat{U}_{\text{band}}|_{\mathcal{N} \setminus \mathcal{R}} = \hat{U}_{\text{band}}^0 + \hat{U}_{\text{band}}^d, \quad \mathcal{S}|_{\mathcal{N} \setminus \mathcal{R}} = \mathcal{S}^{\sigma 0} + \mathcal{S}^{\sigma d} \quad (88)$$

where $\hat{\rho}_0, \hat{U}_{\text{band}}^0$ and $\mathcal{S}^{\sigma 0}$ are piecewise periodic, while $\hat{\rho}^d, \hat{U}_{\text{band}}^d$ and $\mathcal{S}^{\sigma d}$ decay away from the origin. For the interpolation scheme we have:

$$\hat{\rho}_p = \hat{\rho}_p^0 + \sum_{q \in \mathcal{R}} \gamma_p^q (\hat{\rho}_p - \hat{\rho}_q^0), \quad (89)$$

$$\hat{U}_{\text{band}, p} = \hat{U}_{\text{band}, p}^0 + \sum_{q \in \mathcal{R}} \gamma_p^q (\hat{U}_{\text{band}, q} - \hat{U}_{\text{band}, q}^0), \quad (90)$$

$$\mathcal{S}_p^\sigma = \mathcal{S}_p^{\sigma 0} + \sum_{q \in \mathcal{R}} \gamma_p^q (\mathcal{S}_q^\sigma - \mathcal{S}_q^{\sigma 0}), \quad (91)$$

in which $\hat{\rho}_p = \hat{\rho}(\mathbf{x}^p)$, with $p \in \mathcal{N} \setminus \mathcal{R}$, and γ_p^q are the weights determined by the degree of interpolation/approximation used, but also depend on p and q . More information about this

can be found in [Suryanarayana et al.2013] and [Knott2000].

For the electrostatic potential $\tilde{\kappa}$, we use a similar approximation scheme:

$$\tilde{\kappa}|_{\mathcal{N} \setminus \mathcal{R}} = \tilde{\kappa}_0 + \tilde{\kappa}_d. \quad (92)$$

The *perturbation* $\tilde{\kappa}_d$ is evaluated by numerically solving

$$-\frac{1}{4\pi}\Delta_{\mathbf{x}}\tilde{\kappa}_d = \tilde{\rho} - \tilde{\rho}_0 + b - b_0, \quad (93)$$

as has been done for (64) and (65). For $\tilde{\kappa}_0$, a guess will be used.

CGDFT can be summarized in the following algorithm:

Generate guess for positions of the nuclei (\mathbf{R})

repeat

 Calculate charge density of the nucleus $b(\mathbf{x}, \mathbf{R})$, (66);

 Generate the piecewise periodic $\hat{\rho}^0$, \hat{U}_{band}^0 , \mathcal{S}^0 and a guess for $\tilde{\kappa}_0$;

 Generate a guess for electron density $\rho(\mathbf{x})$

for each $\mathbf{x}^p, p \in \{1, \dots, N_d^3\}$ **do**

repeat

 Calculate the electrostatic potential $\tilde{\kappa}(\mathbf{x}, \mathbf{R})$, (64);

 Calculate the exchange correlation potential $V_{\text{XC}}[\hat{\rho}]$, §4.4;

 Discretize the Hamiltonian, (81);

 Calculate spectral quadrature points and weights at representative nodes, (84);

 Calculate the Fermi energy;

 Calculate the electron density $\hat{\rho}$ at representative nodes $\hat{\rho}_q, q \in \mathcal{R}$, (85);

 Interpolate the electron density $\hat{\rho}$ to nodes $\hat{\rho}_p, p \in \mathcal{N} \setminus \mathcal{R}$, (89) ;

 Normalize and update electron density;

until *convergence of the electron density*;

end

 Evaluate the ground-state energy, using (70), (86), (89) and (90);

 Calculate forces on the nuclei, using (63);

until *Energy minimized with respect to position of atoms*;

Evaluate the entropy and Helmholtz free energy, using (87) and (75).

Algorithm 2: CGDFT.

6.4 CGDFT on single atoms

In the previous sections, some approximation steps had not been discussed in detail, but will be here. As CGDFT is applied only on small atoms in this section, all nodes are considered representative nodes. Since all points \mathbf{x}^p are seen as representative nodes, no interpolation scheme is needed and therefore no guess for ρ_0 , u_0 , s_0 and κ_0 as well. Because a single atom only has a single nucleus, the origin is place in the nucleus and the parameter $R = 0$ will be dropped. A linear grid as in (65) is used. We will now discuss each of the steps in Algorithm 2 in detail for atoms.

Calculate the charge density of the nucleus $b(\mathbf{x})$

The charge density of the nucleus can be calculated using (66):

$$b(\mathbf{x}) = -\frac{1}{4\pi} \Delta_{\mathbf{x}} V_{\text{ext}}^{PS}(\mathbf{x}) = -\frac{1}{4\pi} \left(\frac{d^2 V_{\text{ext}}^{PS}(\mathbf{x})}{dx^2} + \frac{d^2 V_{\text{ext}}^{PS}(\mathbf{x})}{dy^2} + \frac{d^2 V_{\text{ext}}^{PS}(\mathbf{x})}{dz^2} \right). \quad (94)$$

An example of such a pseudo-potential V_{ext}^{PS} is the *Evanescent pseudo-potential*. [Fiolhais et al.1995] This potential is given by

$$\omega(\mathbf{x}) := -\frac{Z}{R} \left\{ \frac{R}{|\mathbf{x}|} \left[1 - \left(1 + \beta \frac{|\mathbf{x}|}{R} \right) e^{-\alpha \frac{|\mathbf{x}|}{R}} \right] - A e^{-\frac{|\mathbf{x}|}{R}} \right\}, \quad (95)$$

where

R is the core decay length in a_0 ,

$$\beta = \frac{\alpha^3 - 2\alpha}{4(\alpha^2 - 1)},$$

$$A = \frac{1}{2}\alpha^2 - \alpha\beta,$$

where the *core decay length* is a measure for the length in a_0 in which the electrons have interaction with the core, and α is an experimental parameter. Values for α and R for crystals can be found in [Fiolhais et al.1995]. For $\Delta_{\mathbf{x}} V_{\text{ext}}^{PS}$ we obtain:

$$\begin{aligned} b(\mathbf{x}) = \sum_{a \in \{x, y, z\}} \frac{d^2 V_{\text{ext}}^{PS}(\mathbf{x})}{da^2} &= \frac{Z}{|\mathbf{x}|^3} - |-3Z|\mathbf{x}|^3 + Z \exp(-\alpha|\mathbf{x}|/R) \left[\frac{-1}{|\mathbf{x}|^3} - \frac{3}{|\mathbf{x}|^3} + \frac{\alpha}{R|\mathbf{x}|^2} + \right. \\ &\quad \left. \alpha \left(\frac{1}{R|\mathbf{x}|} + \frac{2}{|\mathbf{x}|^2} + \frac{\alpha}{R^2|\mathbf{x}|} \right) + \beta \alpha \left(\frac{-1}{R^2|\mathbf{x}|} + \frac{1}{R^3|\mathbf{x}|} + \frac{\alpha}{R^3} \right) \right] + \frac{ZA}{R^2} \exp(-|\mathbf{x}|/R) \left[-1 + |\mathbf{x}| + \frac{1}{R} \right]. \end{aligned} \quad (96)$$

Here, $\alpha \in [2.8, 4.2]$ is an experimental parameter and $R \in [0.3, 0.6]$; the heavier an atom, the higher the value for R .

Generate a guess for electron density $\hat{\rho}(\mathbf{x})$

As initial guess for the electron density $\hat{\rho}(\mathbf{x})$, the *Thomas-Fermi approximation* will be used: [Pask2013] we have $\forall p \in \{1, \dots, N_d^3\}$

$$\rho^{TF}(\mathbf{x}^p) = \frac{1}{3\pi^2} \left(\frac{2Z_{\text{eff}}}{|\mathbf{x}^p|} \right)^{3/2}, \quad (97)$$

with

$$Z_{\text{eff}} := Z \left(1 + \xi \sqrt{\zeta} + \mu \zeta \exp(-\nu \sqrt{\zeta}) \right)^2 \exp(-2\xi \sqrt{\zeta}), \quad (98)$$

and $V^{TF}(\mathbf{x}^p)$ an overall potential, with

$$\zeta = r_p \left(\frac{128Z}{9\pi^2} \right)^{1/3}.$$

Furthermore, ξ , μ and ν are numerically obtained:

$$\begin{aligned}\xi &= 0.7280642371, \\ \mu &= -0.5430794693, \\ \nu &= 0.3612163121.\end{aligned}$$

Calculate the electrostatic potential $\tilde{\kappa}(\mathbf{x})$

For the electrostatic potential, the following equation needs to be solved $\forall p \in \{1, \dots, N_d\}$:

$$-\frac{1}{4\pi}\Delta_{\mathbf{x}}\tilde{\kappa}(\mathbf{x}^p) = \hat{\rho}(\mathbf{x}^p) + b(\mathbf{x}^p). \quad (99)$$

For solving this equation numerically, (65) is used and a Poisson solver is used. [poissonsolver]

Calculate the exchange correlation potential V_{XC}

For the exchange correlation potential, the LDA and the definition of r_s from §4.4 are used as in (49).

$$\begin{aligned}V_{XC}^{\text{LDA}}[\hat{\rho}] &= \epsilon_X + \epsilon_C - \frac{r_s}{3} \frac{\delta\epsilon_{XC}[r_s]}{\delta r_s} = \epsilon_X + \epsilon_C - \frac{r_s}{3} \left(\frac{\delta\epsilon_X[r_s]}{\delta r_s} + \frac{\delta\epsilon_C[r_s]}{\delta r_s} \right) \\ &= \epsilon_X[r_s] + \epsilon_C[r_s] - \frac{r_s}{3} \left(\frac{3}{4} \left(\frac{9}{4\pi^2} \right)^{1/3} \frac{1}{r_s^2} + \frac{\gamma \left(\frac{1}{2}\beta_1 \frac{1}{\sqrt{r_s}} + \beta_2 \right)}{(1 + \beta_1 \sqrt{r_s} + \beta_2 r_s)} \right).\end{aligned}$$

Calculate spectral quadrature points and weights at representative nodes, (84)

This is done by using the LSSGQ method, which is described in §6.2.

Calculate the Fermi energy

For calculating the Fermi energy, the following equation needs to be solved, for which the *bisection method* [Trangenstein] will be used on:

$$f(m) = N_e - 2 \sum_{p=1}^{N_d^3} \sum_{k=1}^K \hat{w}_k^p \frac{1}{1 + \exp\left(\frac{\hat{\lambda}_k^p - m}{\sigma}\right)} \stackrel{!}{=} 0, \quad (100)$$

with the following iteration scheme on an interval $[a^0, b^0]$, where $a^0, b^0 \in \mathbb{R}$ with $m^0 := (a^0 + b^0)/2$:

$$\begin{cases} f(m^i) > 0 \rightarrow b^{i+1} := m^i \\ f(m^i) < 0 \rightarrow a^{i+1} := m^i \\ f(m^i) = 0 \rightarrow \lambda_f = m^i, \end{cases}$$

Note that the approximation for $f(m^i) = 0$ has a chosen convergence criterion less than 10^{-8} .

Calculate the electron density at representative nodes $\hat{\rho}, q \in \mathcal{N}$

Since we now have the Fermi energy, the electron density can be calculated by

$$\hat{\rho}_p(\mathbf{x}) = \frac{2}{h^3} \sum_{k=1}^K \hat{w}_k^p \frac{1}{1 + \exp\left(\frac{\hat{\lambda}_k^p - \lambda_f}{\sigma}\right)} \quad (101)$$

Normalize and update electron density

After the electron density is obtained it is normalized as in (69). This is done by approximation the integral for the electron density by Riemann sums and multiplied by a constant such that (69) holds. The Riemann sum \mathcal{R} of a triple integral of the function $f(x, y, z)$ over the partition $[a, b] \times [c, d] \times [e, f]$, is generally defined by:

$$\mathcal{R} \left[\int_a^b \int_c^d \int_e^f f(x, y, z) dx dy dz \right] := \sum_{i=1}^l \sum_{j=1}^m \sum_{k=1}^n f(x_i, y_j, z_k) \Delta x_i \Delta y_j \Delta z_k,$$

with

$$\Delta x_i = x_i - x_{i-1}, \quad \Delta y_j = y_j - y_{j-1}, \quad \Delta z_k = z_k - z_{k-1}.$$

Since we have a linear equidistant grid, $\Delta x_i = \Delta y_j = \Delta z_k = h$. [Math242017] Next the electron density is compared to the electron density in which the iteration started, which was in calculate the electrostatic potential $\tilde{\kappa}\mathbf{x}$. If for each node the difference between the starting electron density and the ending electron density after the loop has an absolute error chosen less than 10^{-8} , the loop is finished and the electron density has converged.

Evaluate the ground-state energy

The ground-state energy is approximated by (70). When using Riemann sums to approximated the integrals, we get for the ground-state energy with

$$\begin{aligned} \mathcal{E}_0^\sigma &\approx 2 \sum_{p=1}^{N_d} \sum_{k=1}^K \hat{w}_k^p \hat{\lambda}_k^p g_\sigma(\hat{\lambda}_k^p; \lambda_f) + h^3 \sum_{i=1}^{N_d} \sum_{j=1}^{N_d} \sum_{k=1}^{N_d} \epsilon_{XC}[\rho]^{i,j,k} \rho^{i,j,k} - \\ &h^3 \sum_{i=1}^{N_d} \sum_{j=1}^{N_d} \sum_{k=1}^{N_d} V_{XC}^{LDA}[\rho]^{i,j,k} \rho^{i,j,k} + \frac{h^3}{2} \sum_{i=1}^{N_d} \sum_{j=1}^{N_d} \sum_{k=1}^{N_d} (b^{i,j,k} - \rho^{i,j,k}) \kappa^{i,j,k} - \\ &\frac{h^6}{2} \sum_{r=1}^{N_d} \sum_{s=1}^{N_d} \sum_{t=1}^{N_d} \sum_{i=1}^{N_d} \sum_{j=1}^{N_d} \sum_{k=1}^{N_d} \frac{b^{i,j,k} b^{r,s,t}}{|x^{i,j,k} - x^{r,s,t}|}. \end{aligned} \quad (102)$$

Because for V_{XC} the LDA is used, this potential is denoted by V_{XC}^{LDA} . After approximating the ground-state energy in Hartree units, it can be converted to electronvolt (eV) by the relation $1 \text{ Ha} = 27.211... \text{ eV}$. [Perdew1981]

Evaluate the entropy and Helmholtz free energy \mathcal{F}

The entropy, \mathcal{S}^σ , of the system is evaluated by (87). After this, the Helmholtz free energy in Hartree units is calculated by using (75).

6.5 CGDFT on a helium atom

The steps described in §6.4 have been implemented in a MATLAB code, which can be found in Appendix A, and has been tested on a helium atom. For helium we have the following parameters:

$$N_e = Z = 2, \quad K = 1, \quad \alpha = 2.9, \quad R = 0.31a_0[\text{Perdew1981}]$$

Furthermore, the experimental ground-state energy value for helium is 2.9037243... Ha. [Li et al.2019] When running the MATLAB code and run it for helium, the following ground-state energy values have been found for different grid sizes. The grid size is the amount of points in the x -direction, y -direction and z -direction, thus the grid itself is a cube of $gridsize \times gridsize \times gridsize$. Note that for example for grid size 19, the origin is at (10, 10, 10).

step size	grid size	energy (Ha)	energy in electronvolts (eV)	computation time (sec.)
0.225	13	-2.668	-72.596	262.270
0.225	15	-2.714	-73.852	662.495
0.225	17	-2.735	-74.430	1641.140
0.225	19	-2.745	-74.693	4101.764
0.225	21	-2.7491	-74.8069	7880.294

Table 2: *Ground-state energy for helium with step size 0.225*

When the grid becomes larger, the total energy is still a bit decreasing. When plotting this, using a power method as interpolating scheme, we obtain the following figure.

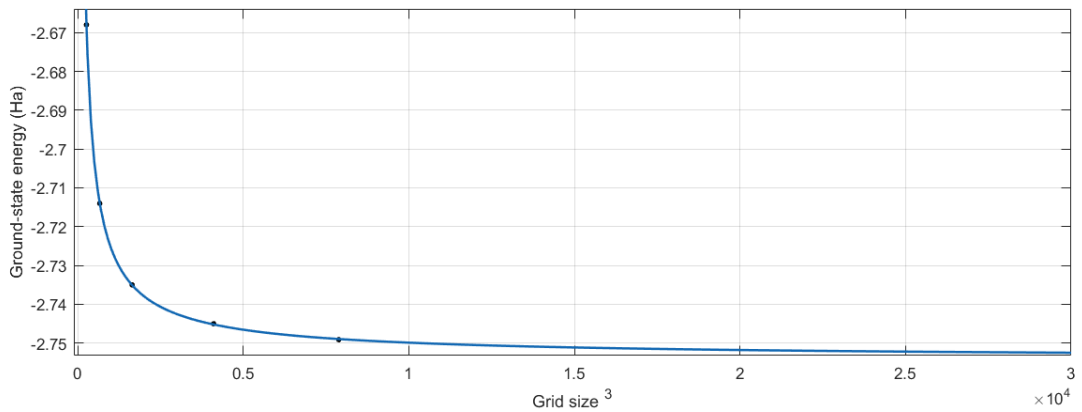


Figure 14: *The number of gridpoints plotted against the ground-state energy.*

However, the downside is that the computation time increases also a lot, especially when looking for over 21 grid points, this leads to more than 2 hours of computing, whereas for the grid size 13 the computation is done within 5 minutes.

When looking for a factor for the computation time, when the grid size is doubled, the computation time becomes approximately 2.5 times as larger. When plotting the number of

6. COARSE-GRAINING DENSITY FUNCTIONAL THEORY

gridpoints against the computation time and using an interpolation scheme, we obtain the following figure

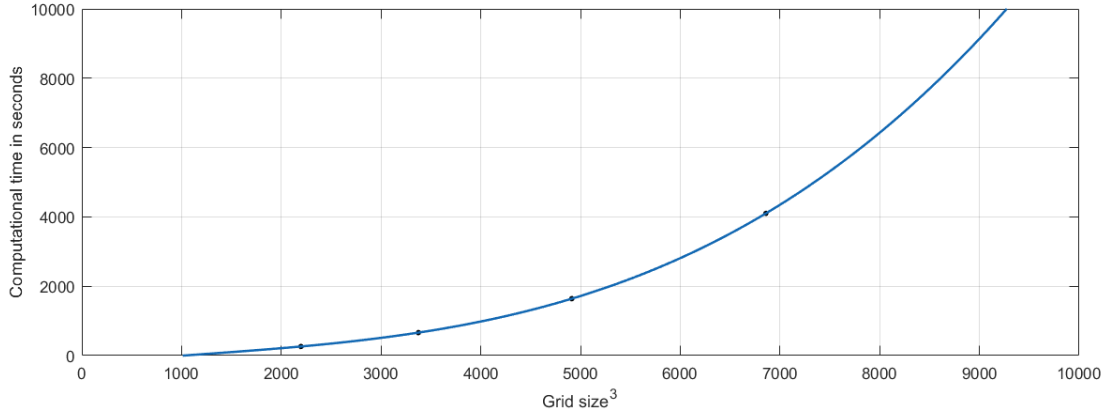


Figure 15: *The number of gridpoints plotted against the computation time in seconds.*

When looking for reasons why the ground state energy differs from the experimental one, a plot is made from the Evanescent Potential compared to the Coulomb Potential $-\frac{2}{|x|}$. This is done, because for large x the Evanescent Potential converges to the Coulomb Potential.

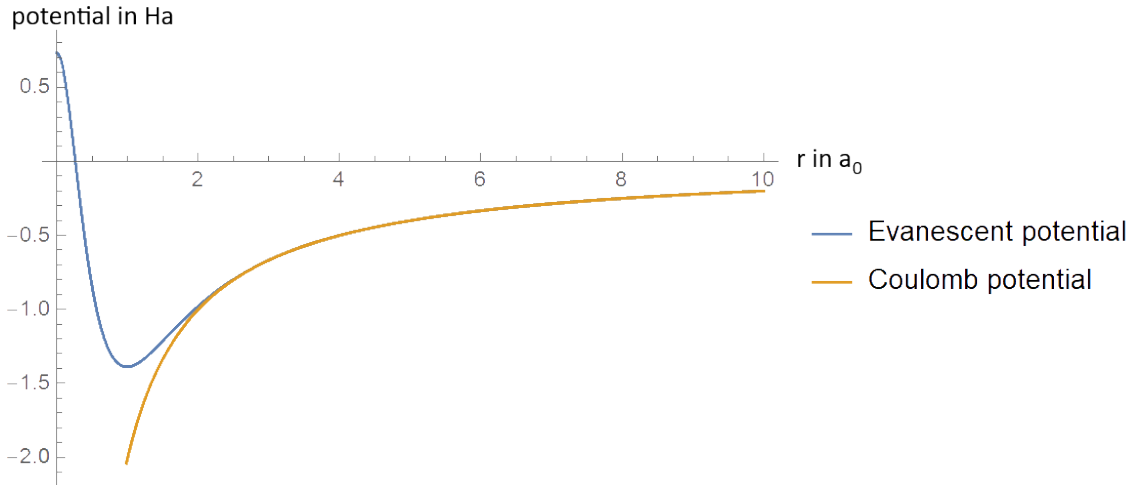


Figure 16: *The Evanescent Potential compared to the Coulomb Potential.*

From this figure, it can be observed that there is a difference between the two for $x \in \langle 0, 4 \rangle$. Because of this difference, the approximated ground state energy is higher than the experimental ground state energy. Furthermore, this difference is also partly done because of the LDA approximation that is used.

When the step size is increased, the ground-state energy increases as well. This is probably due to the fact that around the origin the electron density is higher, but there are too few points to capture this when the step size is too large.

step size	grid size	energy (Ha)	energy in electronvolts (eV)
0.3125	13	-1.611	-43.832
0.3125	15	-1.639	-44.611

Table 3: *Ground-state energy for helium with step size 0.3125*

From this it can be observed that for a too large step size around the origin, the approximation becomes less accurate.

So in conclusion, one is led to think that CGDFT gives a fairly good approximation for the ground-state energy for atoms. The difference could be made less when choosing a different pseudo-potential and a more accurate approximation for V_{XC} than the LDA.

7 Conclusion

In this thesis, we started with an introduction of quantum mechanics in Chapter 2, with the Schrödinger equation as its most important tool. Also, the quantization of classical-mechanical many-particle systems into quantum mechanical systems has been discussed. In Chapter 3, a specific many-particle system has been studied: the hydrogen atom. For the hydrogen atom, quite some computations to find the bound state-energies analytically. Finding exact solutions can only be done in a few cases: this is why numerical approaches are needed. Several ones have been discussed in Chapter 4, among which Density Functional Theory is the most popular one and, formally can give an exact solution. The formulation of DFT by Kohn-Sham has been discussed as well, since the approximations for the kinetic energy were hard to obtain in DFT. An example of Kohn-Sham DFT applied to a carbon atom has been discussed in Chapter 5. However, when one uses Kohn-Sham DFT for larger atoms, the computation time is too large, other methods, refining Kohn-Sham DFT have been considered. An example of such a method is Coarse-Graining DFT.

In Chapter 6, the formulation of CGDFT has been given for molecules, and a reformulation for single atoms after it. In this reformulation, first the charge density of the nucleus is calculated, and a guess for the electron density is made using the Thomas-Fermi approximation. After this, the electron density is calculated for each of the nodes until convergence is reached. For the external potential, the Evanescent pseudo-potential is used. The loop for updating the electron density starts with calculating the electrostatic potential approximation and the exchange correlation potential. Next, the Hamiltonian is discretized and the LSSGQ method is used to compute spectral quadrature points and weights. Then, the Fermi energy is calculated using the bisection method. Having this Fermi energy, an updated electron density can be calculated, and it is compared to the starting density. If the difference is less than 10^{-8} for all nodes, the electron density has been converged, and the loop ends. Now, the ground-state energy can be calculated using Riemann sums to approximate the needed integrals. This algorithm has been implemented in MATLAB, to investigate the method on a atomic scale. By evaluation of the method for a helium atoms, an approximated CGDFT ground-state energy was found. The experimental ground-state energy of helium is -2.9 Ha, compared to the CGDFT approximation of -2.7491 Ha. The difference is mainly caused by the choice of the pseudo-potential and the LDA approximation. Other approximation errors are due to the Riemann sums, a large step size and the bisection method for approximating the Fermi energy. Since the result of the approximated CGDFT ground-state energy is close to the experimental one, it is led to think that CGDFT gives a fairly good result for atoms.

8 Discussion

The CGDFT method has been evaluated for helium, the second smallest atom. For helium, the number of quadrature points is 1: because of this, the Lanczos-iteration makes only use of the initial conditions. In order to investigate the method for slightly larger atoms, like beryllium, where $Z=4$, one can draw a better conclusion whether or not CGDFT gives a close approximation of the ground-state energy value of atoms.

If one would like to have a small step size, one has to compensate this with many grid points and the computation time increases rapidly. So, there is a trade-off between accuracy and computation time, which is a classical one. Furthermore, for helium, where $K = 1$, some computational time was needed, for larger molecules, and thus larger K , this will increase even more. In order to overcome this, one could think of using the distinction of representative and non-representative nodes for atoms to decrease computation time. For metals, $K \ll N_e/2$ in [Suryanarayana et al.2013] it could be found that $K = 20$ already gives good approximations with low errors. This is maybe the case for large atoms as well and it would be interesting to know how many spectral points are needed to obtain a high accuracy compared to the ground-state energy and also having less computational time.

In the algorithm, the Evanescent pseudo-potential is used, which is a local pseudo-potential. In order to investigate the effect of choosing the particular potential, other potentials, like semi-local or global potentials, could be implemented in the algorithm, and the differences can be studied. Also, for the guess of the electron density, another approximation could have been used instead of the Thomas-Fermi approximation. Furthermore, another approximation for the exchange-correlation energy than the LDA could be used. When using the LDA approximation, the approximated ground-state energy will always be slight higher than the experimental one.[Pask2013] If a higher GGA approximation of the approximated ground-state energy will become lower and more towards the experimental one, than with the LDA. Furthermore, the integrals of the potentials are approximated by Riemann sums; when using a more accurate approximation for approximating integrals, one gets closer to the experimental value of the ground-state energy.

For future research, it would also be interesting to know what happens to the ground-state energy, the entropy and the Helmholtz free energy when the temperature changes. Lastly, it would be interesting to see how a change in charge could affect the method. For instance, the effect on the total energy of the calcium atom, having 20 electrons, compared to the Ca^{2+} ion, which has 18 electrons.

References

- [Abramowitz et al.1972] Abramowitz, M., Stegun, I. A., and Miller, D. (1972). *Handbook of Mathematical Functions With Formulas, Graphs and Mathematical Tables*. Courier Corporation, 10 edition.
- [Boyle2010] Boyle, P. A. (2010). 6 wave equation in spherical polar coordinates. Retrieved from https://www2.ph.ed.ac.uk/~paboyle/Teaching/PhysicalMaths/Notes_2010/notes_2010_part3.pdf.
- [Clark2003] Clark, S. (2003). Dirac Exchange.
- [Erhart2016] Erhart, P. (2016). A Very Short Introduction to Density Functional Theory.
- [Fiolhais et al.1995] Fiolhais, C., Perdew, J. P., Armster, S. Q., MacLaren, J. M., and Braczkewska, M. (1995). Dominant Density Parameters and Local Pseudopotentials for Simple Metals. *Physical Review B*, 20:14001–14011.
- [Friedhelm,J and Bechstedt, H2015] Friedhelm,J and Bechstedt, H (2015). Density Function Theory. In *Many-Body Approach to Electronic Excitations*, pages 73–88. Springer-Verlag Berlin Heidelberg, 1 edition.
- [Gustafson and Sigal2011] Gustafson, S. J. and Sigal, I. M. (2011). *Mathematical Concepts of Quantum Mechanics*.
- [Halpern2019] Halpern, J. (2019). 3D Representation of Orbitals. Retrieved from [https://chem.libretexts.org/Bookshelves/General_Chemistry/Map%3A_Chemistry_-_The_Central_Science_\(Brown_et_al.\)/06._Electronic_Structure_of_Atoms/6.6%3A_3D_Representation_of_Orbitals](https://chem.libretexts.org/Bookshelves/General_Chemistry/Map%3A_Chemistry_-_The_Central_Science_(Brown_et_al.)/06._Electronic_Structure_of_Atoms/6.6%3A_3D_Representation_of_Orbitals).
- [Hawking1988] Hawking, S. (1988). *A Brief History of Time*. Bantam Press, 2016 edition.
- [Igmur2017] Igmur, A. (2017). Energy Levels and Transitions Hydrogen Atoms. Retrieved from <https://i.stack.imgur.com/drWvi.png>.
- [Knott2000] Knott, G. (2000). *Interpolating Cubic Splines*. Springer-Verlag.
- [Li et al.2019] Li, J., Drummond, N., Schuck, P., and Olevano, V. (2019). Comparing Many-Body Approaches Against the Helium Atom Exact Solution. *SciPost Phys*.6.
- [Math242017] Math24 (2017). Definition and Properties of Triple Integrals. Retrieved from <https://www.math24.net/definition-properties-triple-integrals/>.
- [Parris2019] Parris, P. E. (2019). Many Particle System.
- [Pask2013] Pask, J. E. (2013). A Robust and General Schrödinger and Dirac Solver for Atomic Structure Calculations. *Atomic Physics*, 184:1777–1791.
- [Rudin1991] Rudin, W. (1991). *Functional Analysis*. Mc Graw Hill, 7 edition.
- [Schr2011] Schr, T. (2011). Numerical methods of solving kohn-sham equations for atoms. (8):1–3. Retrieved from <http://users.wfu.edu/natalie/s11phy752/lecturenote/numericalmethods.pdf>.

REFERENCES

- [Standard2013] Standard, J. (2013). Advantages and Disadvantages of DFT. Retrieved from <https://www.coursehero.com/file/p7oh8ko2/Advantages-and-Disadvantages-of-DFT-One-advantage-of-DFT-is-that-unlike-the/>.
- [Suryanarayana et al.2013] Suryanarayana, P., Bhattacharya, K., and Ortiz, M. (2013). Coarse-Graining Kohn-Sham Density Functional Theory. *Journal of the Mechanics and Physics of Solids*, 61(1):38–60.
- [Wikipedia2010] Wikipedia (2010). Electric Potential & Fields. Retrieved from https://en.wikipedia.org/wiki/Electric_potential.
- [Zunger2018] Zunger, A. (2018). Atomic orbital. Retrieved from https://en.wikipedia.org/wiki/Atomic_orbital#/media/File:Atomic-orbital-clouds_spdf_m0.png.
- [Schrit] T. Schrit, Exploring Atomic Defects in Molybdenum Disulphide Monolayers, *Indian Journal of Physics*, 3(68):159–164. DOI: <https://doi.org/10.1007/s12648-012-0035-0>
- [Young] Young, H.D. , Freedman, R.A., Ford, A.L. (2013) *University Physics with Modern Physics*, Pearson, 14th edition.
- [Masi] Masi, Marco (2018), *Quantum Physics: An Overview of a Weird World*, ISBN:978-1725029569, 2nd edition.
- [Jeffreys1955] Jeffreys, H. (1955). Two Properties of Spherical Harmonics. *Quarterly Journal of Mechanics and Applied Mathematics*, 4(8):448–451. DOI: 10.1093/qjmam/8.4.448
- [Arias2004] Arias, T.A., (2004). Notes on the Ab Initio Theory of Molecules and Solids: Density Functional Theory (DFT). *Journal of Physics*, 480:680.
- [Perdew1981] Perdew, J. P. and Zunger, A. (1981). Self-interaction correction to density-functional approximations for many-electron systems. *Physical Review B*. DOI: 10.1103/PhysRevB.23.5048
- [Ismail-Beigi2000] Ismail-Beigi, Sohrab and Arias, T. A. (2000). New Algebraic Formulation of Density Functional Calculation. *Computer Physics Communications* 128:1–45. DOI: 10.1016/S0010-4655(00)00072-2
- [poissonsolver] Zhang, Kun and Wang, Liangbi and Zhang, Yuwen (2016). Improved Finite Difference Method with a Compact Correction Term for Solving Poissons Equations. *Numerical Heat Transfer, Part B: Fundamentals* 70(5):393–405. DOI: 10.1080/10407790.2016.1215715
- [Trangenstein] Trangenstein, J. (2010). *Scientific Computing*. Springer. 2nd edition.
- [2011AssociatedFunction] Associated Legendre function, (2011),
Retrieved from <http://www.theochem.ru.nl/pwormer/Nowino/nowino.org/wiki/>
- [Urone2019] Urone, P.P. and Hinrichs, R. (2019) The Hydrogen Atom,
Retrieved from <https://phys.libretexts.org/Bookshelves/8.13TheHydrogenAtom>

Appendices

A Matlab program CGDFT on atoms

```
clear all
close all
% initiate states

Zion=2; % Z, atomic number
K = 1; %number of spectral points K,
gridsize = 19
theta =100000; % 273,15 K = 0 C in hartree units, may be very
    high due to conversion
stepgrootte = 36
iternr = 0;
N = 2; %number of electrons
origin = gridsize/2+0.5;
%generate grid
rx = gridsize;
ry = gridsize;
rz = gridsize;
x = zeros(1,rx);
y = zeros(1,ry);
z = zeros(1,rz);

%r = zeros(gridsize , gridsize , gridsize);
Ne = N; %number of electrons
% generate mesh on lineair grid

step = .00625d0*stepgrootte;%

%stepsize in hartree units
for i=1:rx
    x(i)=step*(i-(origin));
end
for i=1:ry
    y(i)=step*(i-(origin));
end
for i=1:rz
    z(i)=step*(i-(origin));
end

%calculate b(r)
alpha =2.9; %dependend on the kind of atom
R = 0.31; %depends on the kind of atom
```

```

zz = Ne; %number of valence electrons

evapotential = zeros(rx,ry,rz);
beta = (alpha^3-2*alpha)/(4*(alpha^2-1));
A = 1/2*alpha^2 - alpha*beta;

bx = zeros(rx,ry,rz);
by = zeros(rx,ry,rz);
bz = zeros(rx,ry,rz);
b = zeros(rx,ry,rz);
%Vext
for i=1:rx
    for j = 1:ry
        for k = 1:rz
            if i== origin && j ==origin && k ==origin
                evapotential(i,j,k)=0;
                b(i,j,k)=0;
            else
                evapotential(i,j,k) = -zz/(R)*(R/((sqrt(x(i)^2+y(j)^2+z(k)^2)))*(1-(1+beta*(sqrt(x(i)^2+y(j)^2+z(k)^2))/(R)))*exp(-alpha*(sqrt(x(i)^2+y(j)^2+z(k)^2))/(R)))-A*exp(-(sqrt(x(i)^2+y(j)^2+z(k)^2))/(R));
                bx(i,j,k) = -3*zz*(x(i))^2*(sqrt(x(i)^2+y(j)^2+z(k)^2))^( -5)+zz*(sqrt(x(i)^2+y(j)^2+z(k)^2))^( -3)+ zz*exp(-alpha*(sqrt(x(i)^2+y(j)^2+z(k)^2))/R)*(-1/(sqrt(x(i)^2+y(j)^2+z(k)^2))^3-3*(x(i))^2/(sqrt(x(i)^2+y(j)^2+z(k)^2))^5+ alpha*(x(i))^2+ alpha*(1/(R*(sqrt(x(i)^2+y(j)^2+z(k)^2))) + 2*(x(i))^2/(sqrt(x(i)^2+y(j)^2+z(k)^2))^4+alpha*(x(i))^2/(R^2*(sqrt(x(i)^2+y(j)^2+z(k)^2))) + beta*alpha*(-1/(R^2*(sqrt(x(i)^2+y(j)^2+z(k)^2))) + (x(i))^2/(R^3*(sqrt(x(i)^2+y(j)^2+z(k)^2))^3 + alpha*(x(i))^2/(R^3*(sqrt(x(i)^2+y(j)^2+z(k)^2))^2))) + zz*A/(R^2*(sqrt(x(i)^2+y(j)^2+z(k)^2)))*exp(-(sqrt(x(i)^2+y(j)^2+z(k)^2))/R)*(-1+(x(i))^2+ (x(i))^2/(R*(sqrt(x(i)^2+y(j)^2+z(k)^2)))));
                by(i,j,k) = -3*zz*(y(j))^2*(sqrt(x(i)^2+y(j)^2+z(k)^2))^( -5)+zz*(sqrt(x(i)^2+y(j)^2+z(k)^2))^( -3)+ zz*exp(-alpha*(sqrt(x(i)^2+y(j)^2+z(k)^2))/R)*(-1/(sqrt(x(i)^2+y(j)^2+z(k)^2))^3-3*(y(i))^2/(sqrt(x(i)^2+y(j)^2+z(k)^2))^5+ alpha*(y(i))^2+ alpha*(1/(R*(sqrt(x(i)^2+y(j)^2+z(k)^2))) + 2*(y(i))^2/(sqrt(x(i)^2+y(j)^2+z(k)^2))^4+alpha*(y(i))^2/(R^2*(sqrt(x(i)^2+y(j)^2+z(k)^2))) + beta*alpha*(-1/(R^2*(sqrt(x(i)^2+y(j)^2+z(k)^2))) + (y(i))^2/(R^3*(sqrt(x(i)^2+y(j)^2+z(k)^2))^3 + alpha*(y(i))^2/(R^3*(sqrt(x(i)^2+y(j)^2+z(k)^2))^2))) + zz*A/(R^2*(sqrt(x(i)^2+y(j)^2+z(k)^2)))*exp(-(sqrt(x(i)^2+y(j)^2+z(k)^2))/R)*(-1+(y(i))^2+ (y(i))^2/(R*(sqrt(x(i)^2+y(j)^2+z(k)^2)))));
            end
        end
    end

```

```

        )^2+ (y(i))^2/(R*(sqrt(x(i)^2+y(j)^2+z(k)^2)))));
    bz(i,j,k) = -3*zz*(z(k))^2*(sqrt(x(i)^2+y(j)^2+z(k)^2))
        ^(-5)+zz*(sqrt(x(i)^2+y(j)^2+z(k)^2))^( -3)+ zz*exp(-
        alpha*(sqrt(x(i)^2+y(j)^2+z(k)^2))/R)*(-1/(sqrt(x(i)
        ^2+y(j)^2+z(k)^2))^3-3*(z(i))^2/(sqrt(x(i)^2+y(j)^2+
        z(k)^2))^5+ alpha*(z(i))^2+ alpha*(1/(R*(sqrt(x(i)
        ^2+y(j)^2+z(k)^2)))) + 2*(z(i))^2/(sqrt(x(i)^2+y(j)
        ^2+z(k)^2))^4+alpha*(z(i))^2/(R^2*(sqrt(x(i)^2+y(j)
        ^2+z(k)^2)))) + beta*alpha*(-1/(R^2*(sqrt(x(i)^2+y(j)
        ^2+z(k)^2))) + (z(i))^2/(R^3*(sqrt(x(i)^2+y(j)^2+z(
        k)^2))^3) + alpha*(z(i))^2/(R^3*(sqrt(x(i)^2+y(j)^2+
        z(k)^2))^2))) + zz*A/(R^2*(sqrt(x(i)^2+y(j)^2+z(k)
        ^2)))*exp(-(sqrt(x(i)^2+y(j)^2+z(k)^2))/R)*(-1+(z(i)
        )^2+ (z(i))^2/(R*(sqrt(x(i)^2+y(j)^2+z(k)^2)))));
    b(i,j,k) = -1/(4*pi)*(bx(i,j,k)+by(i,j,k)+bz(i,j,k));
end
end
end
end

%generate guess for electron density
alpha1 = 0.7280642371;
beta1 = -0.5430794693;
gamma1 = 0.3612163121;
rho = zeros(rx,ry,rz);
for i=1:rx
    for j = 1:ry
        for k = 1:rz
            if i== origin && j == origin && k ==origin
                rho(i,j,k)=0;
            else
                x1= (sqrt(x(i)^2+y(j)^2+z(k)^2))*(128*Zion/(9*pi^2)
                    )^(1/3);
                Zeff= Zion*(1+alpha1*sqrt(x1)+beta1*x1*exp(-gamma1*
                    sqrt(x1)))^2*exp(-2*alpha1*sqrt(x1));
                Vguess= -Zeff/(sqrt(x(i)^2+y(j)^2+z(k)^2));
                rho(i,j,k) = 1/(3*pi^2)*(-2*Vguess)^(3/2);
            end
        end
    end
end

%normalization of rho
t=0;

for i=1:rx
    for j = 1:ry

```

```

        for k = 1:rz
            t = t + rho(i,j,k);
        end
    end
end
t = t*step^3;
tt = t/Zion;

for i=1:rx
    for j = 1:ry
        for k = 1:rz
            rho(i,j,k) = 1/(tt)*rho(i,j,k);
        end
    end
end
end
%end normalization
rhoTF=rho;
rhoinitial = zeros(rx,ry,rz);
convg = false;

while(convg ~= true)
    %set initial rho for comparision at the end
    for i=1:rx
        for j = 1:ry
            for k = 1:rz
                rhoinitial(i,j,k) = rho(i,j,k);
            end
        end
    end
end
%calculate electrostatic potential

Nd = rx*ry*rz;
v = ones(1,Nd-rx);
w = ones(1,Nd-rx^2);
D1 = diag(v,rx);
D2 = diag(v,-rx);
D3 = diag(w,rx^2);
D4 = diag(w,-rx^2);
KK = 1/(step^2).*(full(gallery('tridiag',Nd,1,-6,1))+D1+D2+D3+D4);

rhob = zeros(rx,ry,rz);
for i=1:rx
    for j = 1:ry
        for k = 1:rz
            rhob(i,j,k)= -4*pi*(rho(i,j,k)+b(i,j,k));
        end
    end
end

```

```

        end
    end
    %make a vector of 3Dmatrix rhob.
    rhob = reshape(rhob,[Nd,1]);

    %solve matrix problem KK*kappa=rhob
    kappa = KK\rhob;

    %calculate Vxc and exc
    Vxc = zeros(rx,ry,rz);
    exc= zeros(rx,ry,rz);
    difexc = zeros(rx,ry,rz); %for later use when calculating the
        integrals.
    for i=1:rx
        for j = 1:ry
            for k = 1:rz
                if(rho(i,j,k) <= 0.0d0)
                    Vxc(i,j,k)=0.0d0;
                    exc(i,j,k)=0.0d0;
                elseif(rho(i,j,k) < 3/(4*pi))
                    rs= (3/(4*pi))^(1/3)*(rho(i,j,k))^(−1/3);
                    sqrs=sqrt(rs);
                    gamma2 = −0.1423;
                    beta3 = 1.0529;
                    beta4 = 0.3334;
                    exc(i,j,k) = −3/4*(9/(4*pi^2))^(1/3)/rs + gamma2
                        /(1+ beta3*sqrs+beta4*rs);
                    Vxc(i,j,k) = exc(i,j,k) − rs/3*(3/4*(9/(4*pi^2))
                        ^ (1/3)*1/rs^2 + gamma2*(1/2*beta3*1/sqrs+beta4)
                        /(1+beta3*sqrs + beta4*rs)^2);
                else
                    rs= (3/(4*pi))^(1/3)*(rho(i,j,k))^(−1/3);
                    rsl=log(rs);
                    A = 0.0311;
                    B = −0.048;
                    C = 0.002;
                    D = −0.0116;
                    exc(i,j,k)=−3/4*(9/(4*pi^2))^(1/3)/rs + A*rsl+ B+C*
                        rs*rsl+D*rs;
                    Vxc(i,j,k)= exc(i,j,k) + A*rsl + B −1/3*A + 2/3*C*
                        rs*rsl+1/3*(2*D−C)*rs;
                end;
                difexc(i,j,k)= exc(i,j,k)−Vxc(i,j,k); %for calculating
                    energy
            end
        end
    end
end

```

```

%LSSCGQ method to obtain nodes and weights for each Nd
lambda= zeros(Nd,K);
weights = zeros(Nd,K);
Vxcreshaped = reshape(Vxc,[Nd,1]);
%Vall
V = Vxcreshaped+kappa;
Vmatrix = zeros(Nd,Nd);
for i = 1:Nd
    Vmatrix(i,i) = V(i);
end
Vmatrix;
%for -1/2Delta_x approximation
v = ones(1,Nd-rx);
w = ones(1,Nd-rx^2);
D1 = diag(v,rx);
D2 = diag(v,-rx);
D3 = diag(w,rx^2);
D4 = diag(w,-rx^2);
H = -1/(2*step^2).*(full(gallery('tridiag',Nd,1,-6,1))+D1+D2+D3+D4)
    +Vmatrix;
H;
%start Lanczos iteration

%initialization
v = zeros(Nd,K+2); %normalized version of vv
v(:,1) = zeros(Nd,1);
v(:,2) = zeros(Nd,1);

vv = zeros(Nd,K+2);
vv(:,1) = zeros(Nd,1);
vv(:,2) = zeros(Nd,1);

for p = 1:Nd

    %initialize v2 and vv2
    for i = 1:Nd
        if p==i
            v(p,2)=1;
            vv(p,2)=1;
        end
    end

    bk = zeros(1,K+1);
    bk(1)=1;
    ak = zeros(1,K);

```



```

for i=2:K+1
    ak(i-1) = transpose(v(:,i))*H*v(:,i);
    vv(:,i+1) = (H-ak(i-1)*eye(Nd))*v(:,i)-bk(i-1)*v(:,i-1);
    bk(i)= 1/norm(vv(:,i+1));
    v(:,i+1)= bk(i)*vv(:,i+1);%normalized vector vv
end

Jk = zeros(K);
bk;
ak;
for i=1:K
    Jk(i,i) = ak(i);
end

for i = 2:K
    Jk(i,i-1) = bk(i);
    Jk(i-1,i) = bk(i);
end

%obtain eigenvalues lambda and eigenvectors in W for the weights
[W,L] = eig(Jk);

for i= 1:K
    lambda(p,i)= L(i,i);
    weights(p,i) = W(1,i)^2; %normalized eigenvectors
end

end
lambda;
weights;
%calculate fermi energy

kB = 1.380649*10^(-23)*229388446923097950;
sigma = kB*theta;
sumktoK = zeros(Nd,K);
restvdSom = zeros(1,Nd);
aa = -10000;
bb = 200000;
convg1 = false;
lambdaf = 2;
iter = 0;
maxiter = 10000;
weights;
sumpp = zeros(1,Nd);
%bisection method.
while (convg1 ~= true && iter<maxiter)

```

```

x = (aa+bb)/2;
iter = iter +1;
for p =1:Nd
    sumktoK = zeros(1,K);
    for i = 1:K
        sumktoK(p,i)= weights(p,i)/(1+exp((lambda(p,i)-x)/sigma)
        );
        sumpp(p) = sumpp(p) + sumktoK(p,i);
    end
    restvdSom(p)=(2/step)*sum(sumpp(p));
end
sum(restvdSom);
fx = sum(restvdSom)-Zion;
err = 1*10^(-8);
if abs(fx) < err
    convgl = true;
    lambdaf = x; %fermi energy
else
    if fx <0
        aa = x;
    end
    if fx>0
        bb = x;
    end
end
end
end

%calculate density
hD = step;
rhol= zeros(1,Nd);
summs= zeros(Nd,K);
summs = zeros(1,Nd);
for p = 1:Nd
    for k = 1:K
        %1+exp((lambda(i,k)-lambdaf)/sigma);
        summs(p,k) = weights(p,k)/(1+exp((lambda(p,k)-lambdaf)/
        sigma));
        summs(p) = summs(p) + summs(p,k);
    end
    rhol(p)= 2/(hD)*sum(summs(p));
end

rho = reshape(rhol,[rx,ry,rx]);

%normalization
t=0;

```

```

for i=1:rx
    for j = 1:ry
        for k = 1:rz
            t = t + rho(i,j,k);
        end
    end
end
t = t*step^3;
tt = t/N;

for i=1:rx
    for j = 1:ry
        for k = 1:rz
            rho(i,j,k) = 1/(tt)*rho(i,j,k);
        end
    end
end

voorwaarde = 0;

for i=1:rx
    for j = 1:ry
        for k = 1:rz
            abs(rho(i,j,k)-rhoinitial(i,j,k));
            if abs(rho(i,j,k)-rhoinitial(i,j,k))<1*10^(-8)
                voorwaarde = voorwaarde +1;
            %else
                % abs(rho(i,j,k)-rhoinitial(i,j,k));

            end
        end
    end
end

voorwaarde
iternr = iternr+1;
if voorwaarde == Nd
    convg = true;
else
    convg = false;
end
if iternr==20
    convg = true;
end
%end

```

```

end

Uband = 0;
sumUband1= zeros(Nd,K);
for p = 1:Nd
    for k = 1:K
        sumUband1(p,k) = weights(p,k)*lambda(p,k)/(1+exp((lambda(p,
            k)-lambdaf)/sigma));
        Uband = Uband + sumUband1(p,k);
    end
end
Uband = 2*Uband

eexc = 0;
foutxc = zeros(rx,ry,rz);
for i = 1:rx
    for j = 1:ry
        for k = 1:rz
            foutxc(i,j,k) = rho(i,j,k)*difexc(i,j,k)*step^3;
            eexc = eexc + foutxc(i,j,k);
        end
    end
end
eexc

ekappa =0;
foutekap = zeros(rx,ry,rz);
kappa = reshape(kappa,[rx,ry,rx]);
for i = 1:rx
    for j = 1:ry
        for z = 1:rz
            foutekap(i,j,k) =(b(i,j,k)-rho(i,j,k))*kappa(i,j,k).*
                step^3; %riemann sum to evalute integrals
            ekappa = ekappa + foutekap(i,j,k);
        end
    end
end
ekappa = 1/2*ekappa;

foutmidden = zeros(rx,ry,rz,rx,ry,rz);
fout =0;
for kk = 1:rz
    for jj = 1:ry
        for ii = 1:rx
            for k = 1:rz

```

```

        for j = 1:ry
            for i = 1:rx
                if ii==i && jj ==j && kk==k
                    foutmidden(ii,jj, kk,i,j,k) = 0;
                else
                    foutmidden(ii,jj, kk,i,j,k) = b(ii,jj, kk
                        )*b(i,j,k)*1/sqrt((i-ii)^2+(j-jj)
                        ^2+(k-kk)^2)*step^6;
                    fout = fout + foutmidden(ii,jj, kk,i,j,k
                        );
                end
            end
        end
    end
end
end
end

eoverige = -1/2*fout;

E= Uband+eexc+eoverige+ekappa;

S = 0;
S1= zeros(Nd,K);
for p = 1:Nd
    for k = 1:K
        lambda(p,k)-lambdaf;
        log(1-1/(1+exp((lambda(p,k)-lambdaf)/sigma)));
        exp((lambda(p,k)-lambdaf)/sigma);
        S1(p,k) = weights(p,k)*(1/(1+exp((lambda(p,k)-lambdaf)/
            sigma))*log(1/(1+exp((lambda(p,k)-lambdaf)/sigma)))
            +(1-1/(1+exp((lambda(p,k)-lambdaf)/sigma)))*log(1-1/(1+
            exp((lambda(p,k)-lambdaf)/sigma))));
        S = S + S1(p,k);
    end
end
S = -kB*2*S/0.000003166789688072391;
%S = -kB/(2*pi)*symsum(symsum(weights(p,k)*(1/(1+exp((lambda(p,k)-
    lambdaf)/sigma))*log(1/(1+exp((lambda(p,k)-lambdaf)/sigma)))
    +(1-1/(1+exp((lambda(p,k)-lambdaf)/sigma))*log(1-1/(1+exp((
    lambda(p,k)-lambdaf)/sigma))))),k,1,K),p,1,Nd);
E = E
Eev = 27.2113962*E
theta = 0.000003166789688072391*theta;
F = E-theta*S%free energy
iternr =iternr

```

```
S= S  
F;  
E0 = 1/2*(E+F);  
colormap('hot')  
imagesc(rho)
```